

Transformable *Cis-trans* Isomerism of Ruthenium (II) Complexes with Photoactivated Anticancer Activity

Chen Pan,^{‡ a} Pui-Yu Ho,^{‡ a,b} Wan-Qiong Huang,^a Gui-Feng Huang,^a Li-Hua Zhang,^b Daniel Nnaemaka Tritton,^d Shek-Man Yiu,^c Wai-Lun Man,^d Chi-Chiu Ko,^c Chi-Fai Leung,^{*b} and Wen-Xiu Ni^{*a}

^a Department of Medicinal Chemistry, Shantou University Medical College, Shantou, Guangdong, 515041, P. R. China. E-mail: wxni@stu.edu.cn, ORCID: 0000-0002-2370-6300

^b Department of Science and Environmental Studies, The Education University of Hong Kong, 10 Lo Ping Road, Tai Po, New Territories, Hong Kong, China. Email: cfleung@eduhk.hk, ORCID: 0000-0003-2830-0737

^c Department of Chemistry, City University of Hong Kong Tat Chee Avenue, Kowloon, Hong Kong, China.

^d Department of Chemistry, Hong Kong Baptist University Waterloo Road, Kowloon, Hong Kong, China.

‡ C. Pan and P. Ho contributed equally to this work.

Table of Contents

TABLE OF CONTENTS	1
EXPERIMENTAL PROCEDURES	4
Synthesis and Characterizations.....	4
Spectroscopic Studies for the Photoisomerization of C1	6
Photoisomerization of C1 was further studied using ¹ H NMR.	6
Cyclic Voltammetry	7
HPLC Determination.....	7
X-ray Crystallography	7
Cell Culture	7
Cytotoxicity analysis	8
Cell colony formation analysis.....	8
Apoptosis analysis	8
Reactive oxygen species analysis	8
LDH release analysis	9
Hoechst 33258 staining analysis	9
Cellular GSH analysis	9
Western blot analysis	9
Animal experiments	10
Animal liver and kidney function analysis	10
Histopathological analysis	10
Photo-activated Anti-tumor Activity of C1 in vivo.....	11
TABLES	12
Table S1. Summary of νN≡C for complexes C1 – C3 and T1 – T3	12
Table S2. Summary of crystal and structural determination data for C3 and T3	12
Table S3. Selected bond lengths (Å) and bond angles (°) of T3 and C3	13
Table S4. ESI-MS data obtained for the photoisomerization of C1 to T1 after irradiated by white LED (λ>420 nm, obtained from PRIME LED) for 15 min in DMSO/H ₂ O (9:1) after 30 min.	13
Table S5. Cytotoxicity values (IC ₅₀ /μM) for 72h of C1 – C3 and T1 – T3 towards human cells in dark.....	13
Table S6. ESI-MS data obtained for the reaction of GSH (1 mM) with T1 (100 μM) in DMSO/ CH ₃ OH/H ₂ O (1:17:2) after 1 hour.....	14
Table S7. ESI-MS data obtained for the reaction of GSH (1 mM) with C1 (100 μM) in DMSO/ CH ₃ OH/H ₂ O (1:17:2) after 30 min irradiation by white LED (λ>420 nm, obtained from PRIME LED).	14
FIGURES	15
Figure S1. Overlaid absorption spectra of C1 – C3 (a) and T1 – T3 (b) in CH ₂ Cl ₂	15

SUPPORTING INFORMATION

Figure S2. CVs of C1 – C3 and T1 – T3 in 0.1M [ⁿ Bu ₄ N]PF ₆ solution in dichloromethane under Ar. Scan rate = 100 mV s ⁻¹	16
Figure S3. Perspective drawings of C3 (left) and T3 (right). Thermal ellipsoids are drawn at 50% probability (hydrogen atoms are omitted for clarity).	16
Figure S4. Absorption spectral change of 40μM C1 – C3 and T1 – T3 in DMSO in dark, respectively.	17
Figure S5. ¹ H NMR spectrum of T1 in d-Dichloromethane.	18
Figure S6. ¹ H NMR spectrum of T2 in d-Dichloromethane.	18
Figure S7. ¹ H NMR spectrum of T3 in d-Dichloromethane.	19
Figure S8. ¹ H NMR spectrum of C1 in d-Dichloromethane.	19
Figure S9. ¹ H NMR spectrum of C2 in d-Dichloromethane.	20
Figure S10. ¹ H NMR spectrum of C3 in d-Dichloromethane.	20
Figure S11. ¹³ C NMR spectra of T3 in d-Dichloromethane.	21
Figure S12. ¹³ C NMR spectrum of C3 in d-Dichloromethane.	21
Figure S13. ATR-FTIR spectra of T1 (left) and C1 (right).	22
Figure S14. ATR-FTIR spectra of T2 (left) and C2 (right).	22
Figure S15. ATR-FTIR spectra of T3 (left) and C3 (right).	23
Figure S16. ESI-MS spectra of T1 and C1 in CH ₂ Cl ₂ , respectively.	24
Figure S17. ESI-MS spectra of T2 and C2 in CH ₂ Cl ₂ , respectively.	25
Figure S18. ESI-MS spectra of T3 and C3 in CH ₂ Cl ₂ , respectively.	26
Figure S19. Overlaid UV/vis absorption spectra of T1 (0.033 mM), C1 (0.033mM) in CH ₂ Cl ₂ and the product isolated from photoisomerization of C1 after irradiation (1 hr) using white LED lamp (λ>420 nm, obtained from PRIME LED). Percentage conversion determined by the extinction coefficient (ε = 42000 M ⁻¹ cm ⁻¹) and absorbance of peak at 326 nm (T1).	27
Figure S20. IR spectra of the isolated product after photoisomerization of C1 (1 mM) in CH ₂ Cl ₂ irradiated with white LED (λ > 420 nm, max. 471 nm, obtained from PRIME LED). under air (a) and Ar (b).	28
Figure S21. UV/vis absorption spectral change of T1 (0.1 mM) in CH ₂ Cl ₂ upon irradiation with white LED (λ > 420 nm, max. 471 nm, obtained from PRIME LED).	29
Figure S22. (a) Formation of T1 as estimated by absorbance at 520 nm during first 6 min of photoisomerization (white LED lamp, λ > 420 nm, max. 471 nm, obtained from PRIME LED) with varied [C1] in CH ₂ Cl ₂ saturated with Ar at 25 °C. (b) Plot of k _{obs} against [C1]; slope = 8.1552×10 ⁻⁴ ± 3.5517×10 ⁻⁵ , y-intercept = 3.3555×10 ⁻⁵ ± 1.9419×10 ⁻⁶ , R ² = 0.996.	29
Figure S23. Spectral change of upon irradiation of C1 (0.0342 – 0.0717 mM) in CH ₂ Cl ₂ with white LED light (λ > 420 nm, max. 471 nm, obtained from PRIME LED). Inset: change in absorbance at 520 nm and estimated concentration T1 produced.	30
Figure S24. ¹ H-NMR spectra of T1 (4 mM) in CD ₂ Cl ₂ upon irradiation with white LED (λ > 420 nm, max. 471 nm, obtained from PRIME LED) at different time (0 – 120 min) under an Ar atmosphere.	30
Figure S25. The absorption spectrum changes of 20 μM C1 in the dark with 5% DMSO in PBS.	31

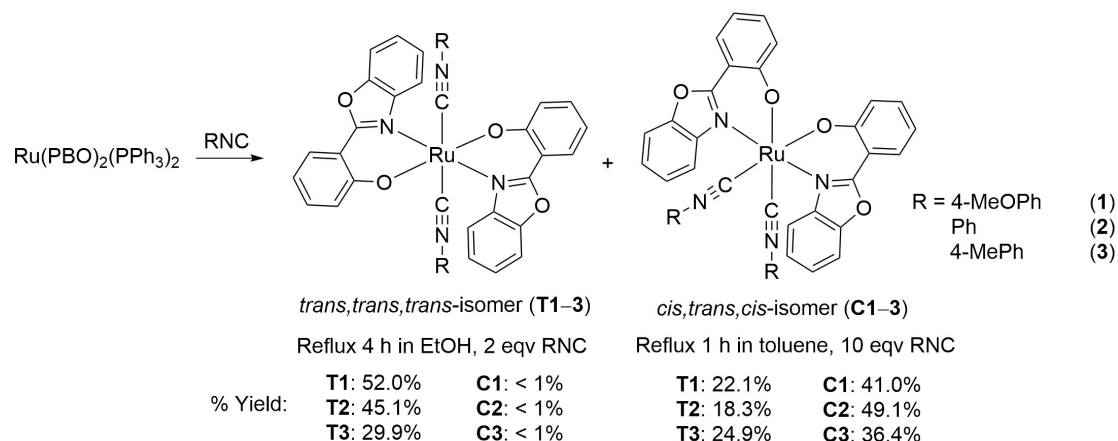
SUPPORTING INFORMATION

Figure S26. The absorption spectrum changes of 20 μ M C1 in 5% DMSO in PBS after irradiation ($\lambda=420$ nm, 50.31 mW/cm ² , 40 min).....	31
Figure S27. The absorption spectrum changes of 20 μ M T1 in the dark with 5% DMSO in PBS.....	32
Figure S28. The absorption spectrum changes of 20 μ M T1 in 5% DMSO in PBS after irradiation ($\lambda=420$ nm, 11.07 mW/cm ² , 10 min).....	32
Figure S29. Stability of C1 in mixed solvent DMSO/ACN/PBS (1:49:50, v/v/v) in the dark determined by HPLC.....	33
Figure S30. Spectral change upon irradiation of C1 (0.02 mM) in DMSO/H ₂ O (9:1) white LED ($\lambda > 420$ nm, max. 471 nm, obtained from PRIME LED). (black line time interval = 1 min). Spectrum of T1 (0.02 mM) (cyan dot line) after 30 min irradiation.....	33
Figure S31. ESI-MS spectra of C1 (0.02 mM) in DMSO/H ₂ O (9:1) after being irradiated for 30 min with white LED ($\lambda > 420$ nm, max. 471 nm, obtained from PRIME LED). Inset: simulated and experiment isotopic patterns of the peaks at $m/z = 734.09$ and 834.09 respectively.....	34
Figure S32. ESI-MS spectra of GSH (1 mM) with C1 (0.1 mM) in DMSO/CH ₃ OH/H ₂ O (1:17:2) after being irradiated for 30 min with white LED ($\lambda > 420$ nm, max. 471 nm, obtained from PRIME LED). Inset: simulated and experiment isotopic patterns of the peaks at $m/z = 867.09$, 734.09 and 688.10 respectively.	34
Figure S33. Staining of NCI-H460 cells with Hoechst 33258 after treatment with T1 (5, 10 and 20 μ M) for 48h and were imaged by ZEISS Observer A1 microscope. (Scale bar=100 μ m).....	35
Figure S34. The expression levels change of protein of NCI-H460 cells after treatment with T1 (5, 10 and 20 μ M) for 48 h by western blot assay.	35
Figure S35. Effect of T1 on liver and kidney function in the BALB/c nude mice xenograft model. The levels of AST, ALT, BUN and CRE were detected by serum. (A) AST. (B) ALT. (C) BUN. (D) CRE. The data are shown as means \pm SD. * $p < 0.05$, ** $p < 0.01$, ns $p > 0.05$ vs control group.....	36
Figure S36. The effect of T1 on the histopathologic changes of mice organ tissues was evaluated by H&E staining. Representative images of liver, heart, lung, kidney and spleen of mice in control group, T1 treatment group (8 mg/kg) and cisplatin treatment group (3 mg/kg). (Scale bar=100 μ m)	37
Figure S37. Photo-activate anti-tumor activities in vivo. Representative photos of mice bearing NCI-H460 cells after treatment with C1	37
REFERENCES	37

Experimental Procedures

Synthesis and Characterizations

All chemicals and solvents were of reagent grade and used without further purification. 2-(2-hydroxyphenyl)benzoxazole (Sigma Alrich) and ruthenium (III) chloride hydrate (Strem Chemical Company) were obtained commercially. The complexes $\text{Ru}(\text{PBO})_2(\text{RNC})_2$ were prepared by modifying the previously reported method by reaction of the isocyanides (RNC) and $\text{Ru}^{\text{II}}(\text{PBO})_2(\text{PPh}_3)_2$ under different conditions.¹



Scheme S1. Synthetic Scheme for **T1 – T3** and **C1 – C3**.

The starting material $\text{Ru}(\text{PBO})_2(\text{PPh}_3)_2$ and RNC ligands was obtained by reported procedure.¹ All other chemicals and solvents were commercially obtained and used without further purification.

The isocyanide ligand (2.2 mole equiv.) was added to a suspension of $\text{Ru}(\text{PBO})_2(\text{PPh}_3)_2$ (60 mg, 0.057 mmol) in ethanol (15 mL) under an argon atmosphere. The resulting mixture was refluxed for 4 h, during which the solution gradually turned orange, and a reddish-orange solid was formed. The reddish-orange solid collected by filtration. The *trans,trans,trans*-isomers (**T1 – T3**) was eluted as the major product by column chromatography (silica gel) as the first red major band using dichloromethane and dried in vacuo. Analytically pure complexes were obtained (Yield: 29.9 – 52.0%) as reddish orange microcrystalline solids by recrystallization from dichloromethane/n-hexane. A small amount (Yield: <1%) of the *cis, trans, cis*-isomers (**C1 – C3**) was obtained from the filtrate by column chromatography (neutral alumina) using dichloromethane/ethyl acetate (10:1) as the eluent. Recrystallization from diethyl ether in the dark give analytically pure yellow microcrystalline solids.

Alternatively, the products can also be obtained by a similar procedure by reacting $\text{Ru}(\text{PBO})_2(\text{PPh}_3)_2$ (60 mg, 0.057 mmol) with an excess of isocyanide (10 mole equiv.) in toluene. The mixture was refluxed for an hour, resulting in a clear yellow solution. The solvent was dried in vacuo and the residue was redissolved in dichloromethane and loaded onto a neutral alumina column. The *trans,trans,trans*-isomers (**T1 – T3**) band eluted with dichloromethane as the first red band, while *cis, trans, cis*-isomers (**C1 – C3**) was eluted later as a yellow band using dichloromethane/ethyl acetate (10:1) as a yellow. Analytically pure products were obtained (**C1 – C3**, Yield: 36.4 – 49.1 %) and (**T1 – T2**, Yield: 35.8 – 50.1 %) by recrystallization as above.

SUPPORTING INFORMATION

Characterization of *cis,trans,cis*-[Ru(PBO)₂(4-MeOPhNC)₂] (C1).

Yield: 18.5 mg (41.0%). ¹H NMR (400 MHz, CD₂Cl₂): δ 8.13–8.03 (m, 2H, PBO), 7.90 (dd, *J* = 8.0, 1.9 Hz, 2H, PBO), 7.70–7.60 (m, 2H, PBO), 7.49–7.37 (m, 4H, PBO), 7.11–6.98 (m, 6H, PBO + MeOPhNC), 6.85–6.75 (m, 4H, MeOPhNC), 6.51 (ddd, *J* = 8.0, 6.8, 1.1 Hz, 2H, PBO), 6.33 (dd, *J* = 8.5, 1.2 Hz, 2H, PBO), 3.77 (s, 6H, MeOPhNC). ¹³C NMR (101 MHz, CD₂Cl₂): δ 170.89, 165.55, 162.37, 158.84, 149.66, 142.56, 133.39, 128.15, 127.06, 124.88, 124.81, 122.89, 122.76, 118.31, 114.46, 113.36, 112.37, 110.85, 55.53. Anal. Calcd for C₄₂H₃₀N₄O₆Ru·2H₂O: C, 61.23; H, 4.16; N, 6.80. Found: C, 61.00; H, 3.82; N, 6.74. IR (KBr, cm⁻¹): 2057, 2119 ν (N≡C). UV/vis (CH₂Cl₂) λ_{max}, nm (ε, M⁻¹ cm⁻¹): 325 (41000), 422 (16500). ESI-MS: *m/z* 788 [M]⁺. HRMS Calcd for C₄₂H₃₀N₄O₆Ru [M + H]⁺: *m/z* 789.1287. Found: *m/z* 789.1268.

Characterization of *cis,trans,cis*-[Ru(PBO)₂(PhNC)₂] (C2).

Yield: 20.5 mg (49.1%). ¹H NMR (400 MHz, CD₂Cl₂): δ 8.17–8.09 (m, 2H, PBO), 7.95 (dd, *J* = 8.0, 1.7 Hz, 2H, PBO), 7.69 (dd, *J* = 6.3, 2.6 Hz, 2H, PBO), 7.52–7.42 (m, 4H, PBO), 7.40–7.26 (m, 6H, PhNC), 7.19–7.12 (m, 4H, PhNC), 7.08 (ddd, *J* = 8.6, 7.0, 1.8 Hz, 2H, PBO), 6.58 (dd, *J* = 10.9, 3.9 Hz, 2H, PBO), 6.40 (d, *J* = 8.5 Hz, 2H, PBO). ¹³C NMR (101 MHz, CD₂Cl₂): δ 170.87, 167.40, 162.41, 149.67, 142.43, 133.51, 129.72, 129.38, 128.18, 127.74, 125.83, 124.95, 124.91, 122.86, 118.24, 113.51, 112.35, 110.91. Anal. Calcd for C₄₀H₂₆N₄O₄Ru·4H₂O: C, 60.07; H, 4.28; N, 7.01. Found: C, 60.27; H, 4.00; N, 6.66. IR (KBr, cm⁻¹): 2063, 2127 ν (N≡C). UV/vis (CH₂Cl₂) λ_{max}, nm (ε, M⁻¹ cm⁻¹): 324 (31700), 354 (21800), 418 (15200). ESI-MS: *m/z* 728 [M]⁺. HRMS calcd for C₄₀H₂₆N₄O₄Ru [M + H]⁺: *m/z* 729.1075. Found: *m/z* 729.1060.

Characterization of *cis,trans,cis*-[Ru(PBO)₂(4-MePhNC)₂] (C3)

Yield: 15.7 mg (36.4%). ¹H NMR (400 MHz, CD₂Cl₂) δ 8.03 (d, *J* = 25.6 Hz, 2H), 7.85 (d, *J* = 24.1 Hz, 2H), 7.59 (d, *J* = 26.2 Hz, 2H), 7.37 (dd, *J* = 27.1, 3.9 Hz, 4H), 7.02 (td, *J* = 30.3, 28.8, 14.4 Hz, 8H), 6.56 – 6.38 (m, 2H), 6.37 – 6.19 (m, 2H), 2.27 (d, *J* = 31.1 Hz, 6H). ¹³C NMR (101 MHz, CD₂Cl₂): 170.65, 162.35, 149.64, 142.50, 138.17, 133.40, 129.87, 128.14, 127.17, 125.57, 124.90, 124.84, 122.81, 118.28, 113.47, 112.39, 110.85, 70.75. Anal. Calcd for C₄₂H₃₀N₄O₄Ru: C, 66.75; H, 4.00; N, 7.41. Found: C, 66.44; H, 3.99; N, 7.37. IR (ATR, cm⁻¹): 2125, 2069 ν (C≡N). UV/vis (CH₂Cl₂) λ_{max}, nm (ε, M⁻¹ cm⁻¹): 320 (34800), 419 (14900). ESI-MS: *m/z* 757. [M+H]⁺.

Characterization of *trans,trans,trans*-[Ru(PBO)₂(4-MeOPhNC)₂] (T1).

Yield: 23.5 mg (52.0%). ¹H NMR (400 MHz, (CD₂Cl₂): δ 8.56 (d, *J* = 7.8 Hz, 2H, PBO), 7.93 (d, *J* = 7.6 Hz, 2H, PBO), 7.60 (d, *J* = 7.8 Hz, 2H, PBO), 7.40 (dt, *J* = 15.1, 7.3 Hz, 4H, PBO), 7.22 (t, *J* = 7.2 Hz, 2H, PBO), 6.95 (d, *J* = 8.8 Hz, 4H, MeOPhNC), 6.89 (d, *J* = 8.2 Hz, 2H, PBO), 6.75 (d, *J* = 8.8 Hz, 4H, MeOPhNC), 6.57 (s, 2H, PBO), 3.76 (s, 6H, MeOPhNC). ¹³C NMR (101 MHz, CD₂Cl₂): δ 160.57, 159.36, 149.66, 149.46, 143.30, 132.52, 130.69, 128.58, 127.76, 124.42, 122.92, 122.82, 120.92, 119.70, 114.30, 113.29, 110.70, 109.95, 55.44. IR (KBr, cm⁻¹): 2087 ν (C≡N). Anal. Calcd for C₄₂H₃₀N₄O₆Ru: C, 64.03; H, 3.84; N, 7.11. Found: C, 64.25; H, 3.59; N, 6.72. UV/vis (CH₂Cl₂) λ_{max}, nm (ε, M⁻¹ cm⁻¹): 326 (31800), 445 (4300). ESI-MS: *m/z* 787.6 [M]⁺. HRMS calcd for C₄₂H₃₀N₄O₆Ru [M]⁺: *m/z* 788.1209. Found: *m/z* 788.1204.

Characterization of *trans,trans,trans*-[Ru(PBO)₂(PhNC)₂] (T2).

Yield: 18.8 mg (45.1%). ¹H NMR (400 MHz, (CD₂Cl₂): δ 8.57 (d, *J* = 7.1 Hz, 2H, PBO), 7.94 (dd, *J* = 8.0, 1.3 Hz, 2H, PBO), 7.61 (d, *J* = 7.7 Hz, 2H, PBO), 7.41 (dtd, *J* = 21.1, 7.5, 1.2 Hz, 4H, PBO), 7.33–7.19 (m, 8H, PBO + PhNC), 7.08–6.97 (m, 4H, PhNC), 6.91 (d, *J* = 8.5 Hz, 2H, PBO), 6.58 (t, *J* = 7.2 Hz, 2H, PBO). ¹³C NMR (101 MHz, CD₂Cl₂): δ 173.19, 160.66, 149.66, 143.22, 137.29, 132.66, 129.18, 128.64, 128.47, 128.03, 126.45, 124.49, 124.46, 122.84, 119.66, 113.38,

SUPPORTING INFORMATION

112.72, 110.00. IR (KBr, cm^{-1}): 2080 ν ($\text{C}\equiv\text{N}$). Anal. Calcd for $\text{C}_{40}\text{H}_{26}\text{N}_4\text{O}_4\text{Ru}$: C, 66.02; H, 3.60; N, 7.70. Found: C, 66.33; H, 3.37; N, 7.37. UV/vis (CH_2Cl_2) λ_{max} , nm (ϵ , $\text{M}^{-1}\text{cm}^{-1}$): 331 (24400), 444 (4200). ESI-MS: m/z 728.2 $[\text{M}]^+$. HRMS calcd for $\text{C}_{40}\text{H}_{26}\text{N}_4\text{O}_4\text{Ru}$ $[\text{M}]^+$: m/z 728.0998. Found: m/z 728.0994

Characterization of *trans,trans,trans*-Ru(PBO)₂(4-MePhNC)₂ (T3)

Yield: 12.9 mg (29.9%). ¹H NMR (400 MHz, CD_2Cl_2) δ 8.52 (dd, $J = 7.7, 1.6$ Hz, 2H), 7.88 (dd, $J = 8.2, 1.8$ Hz, 2H), 7.56 (dd, $J = 7.9, 1.4$ Hz, 2H), 7.41 – 7.30 (m, 4H), 7.17 (ddd, $J = 8.7, 6.8, 1.9$ Hz, 2H), 7.02 (d, $J = 8.2$ Hz, 4H), 6.85 (dd, $J = 8.6, 2.2$ Hz, 6H), 6.53 (t, $J = 7.5$ Hz, 2H), 2.26 (s, 6H). ¹³C NMR (101 MHz, CD_2Cl_2): 149.66, 143.22, 139.00, 129.71, 126.17, 124.42, 119.68, 109.94. Anal. Calcd for $\text{C}_{42}\text{H}_{30}\text{N}_4\text{O}_4\text{Ru}$: C, 66.75; H, 4.00; N, 7.41. Found: C, 66.68; H, 3.76; N, 7.14. IR (ATR, cm^{-1}): 2073 ν ($\text{C}\equiv\text{N}$). UV/vis (CH_2Cl_2) λ_{max} , nm (ϵ , $\text{M}^{-1}\text{cm}^{-1}$): 320 (38900), 445 (6630). ESI-MS: m/z 756 $[\text{M}]^+$.

Spectroscopic Studies for the Photoisomerization of C1

Photoisomerization was performed using a dichloromethane solution of **C1** (1 mM, 3 mL) in a pyrex tube (volume = 12.4 mL) with ground-joint. The tube was sealed with a rubber septum and the solution was Ar-purged for 15 min. The solution was irradiated by a LED lamp (White LED lamp, >420 nm, is obtained from PRIME LED with 18 bulbs and total intensity of 486 mW, and attached on a double-walled glass water jacket beaker with water circulation). Samples are placed at center of the water jacket with 3.5 cm distance to the light bulbs. A portion of the solution (0.1 mL) was then withdrawn and concentrated by rotary evaporator, photoisomerization product (**T1**) was isolated by column chromatography on silica gel with CH_2Cl_2 as eluent. The **T1** isolated was redissolved in fixed amount of CH_2Cl_2 (3 mL, dilution factor = 30). Percentage (%) conversion of **C1** to **T1** was determined by UV/vis spectroscopy (Agilent Cary 8454 UV/vis) and estimated using the following equation:

$$\% \text{ conversion} = \frac{A_{T1}}{a_{T1}} \div [\text{C1}] \times \text{dilution factor} \times 100\%$$

Where A_{T1} is the absorbance at 326 nm for the isolated product solution, a_{T1} is absorptivity of **T1** at 326 nm ($\epsilon = 42000 \text{ M}^{-1}\text{cm}^{-1}$) and $[\text{C1}]$ is the initial concentration of **C1**. Absorption spectra of 0.033 mM **T1** (100% conversion) solution is included in Figure S4 for comparison. UV/vis absorption spectral change (Figure 1A) was collected similarly, using an Ar-purged CH_2Cl_2 solution (0.1 mM, 3 mL) of **C1** in a quartz cuvette sealed with a rubber septum. Absorption spectra were collected at regular time interval (1 min) and $[\text{T1}]$ was estimated by absorptivity of **T1** at 520 nm ($\epsilon = 2500 \text{ M}^{-1}\text{cm}^{-1}$).

Photoisomerization was also monitored by FT-IR spectroscopy (PerkinElmer Frontier FT-IR Spectrometer, equipped ATR sampling) using a 1 mM CH_2Cl_2 solution of **C1** as above. A fresh solution of the isolated product was dropped on the ATR sampling and the spectra were collected after the sample solution is completely air-dried.

Photoisomerization of C1 was further studied using ¹H NMR.

Solutions of **T1** and **C1** (4 mM) in Ar-purged CD_2Cl_2 (Sigma Aldrich) were prepared in NMR tubes sealed with a rubber septum, and the initial proton spectra of the respective complexes were recorded before irradiation. Then the solution was irradiated with a LED lamp (white, $\lambda > 420$ nm; max. 471nm) and the ¹H NMR spectra was acquired at different

SUPPORTING INFORMATION

time by quickly placing the NMR tubes in the NMR spectrometer (Bruker Avance III UltraShield Magnett 400 MHz Fourier Transform NMR).

Cyclic Voltammetry

Cyclic voltammetry (CV) was performed on a Zahner Zennium Electrochemical Workstation using a glassy-carbon working electrode (3 mm), a Pt-wire counter electrode and a SCE reference electrode. Before the CVs were collected, CH₂Cl₂ solutions of the complexes containing 0.1M ⁿBu₄NBF₄ as the supporting electrolyte were purged with Ar for at least 15 min. ⁿBu₄NBF₄ was recrystallized for three times from hot ethanol and dried in vacuo before used. Ferrocene (Fc⁺/Fc) was used as the internal reference in all measurements. CH₂Cl₂ was of HPLC grade (Anaqua) and used without further purification.

HPLC Determination

The stability of **C1** in DMSO/ACN/PBS (1:49:50, v/v/v) in dark was investigated by High-performance liquid chromatography (HPLC). HPLC profiles were performed on an Agilent 1260 HPLC system equipped with an Poroshell 120 EC-C18 column (4.6 × 100mm, 4 μm). The mobile phase was a gradient elution of acetonitrile/water (70/30, v/v). The flow rate was 1.0 mL/min and the detected wavelength was 254 nm.

X-ray Crystallography

X-ray diffraction data were corrected on a Bruker D8 Venture Photon II Single Crystal XRD using graphite-monochromated Mo-Kα (λ = 0.71073 Å) in the ω-φ scan mode. Data was corrected for absorption effects using the Multi-Scan method (SADABS). The structures were solved and refined using the Bruker SHELXTL Software Package and refined by full-matrix least squares on F² using SHELXL-2016/6². All non-hydrogen atoms were refined anisotropically and H atoms were generated by the program SHELXT 2014/5³. The positions of H atoms were determined on basis of a riding mode. The crystal data and experimental details are summarized in **Table S2**. CCDC no. 2378681-2378682 contain the supplementary crystallographic data for this paper.

Cell Culture

The human cell lines A549 and NCI-H460 (both human lung cancer cells), Hela (human cervical cancer cells), MDA-MB-231 (human breast cancer cells), HFL1 (human lung fibroblasts cells) were incubated at 5% carbon dioxide and 37°C in a humidified incubator. The NCI-H460 cell lines were cultured in the RPMI-1640 medium (Gibco, USA), A549, Hela and MDA-MB-231 cell lines in were cultured in the Dulbecco's modified Eagle medium (Gibco, USA) with a low content of glucose (1 g/L) concentration, HFL1 cell lines were cultured in Ham's F-12K (Kaighn's) Medium (Gibco, USA). Both cell lines were cultured in medium supplemented with 10% fetal bovine serum (FBS; Gibco, USA), 2 mM L-glutamine (Gibco, USA) and 1% penicillin/streptomycin (Gibco, USA).

SUPPORTING INFORMATION

Cytotoxicity analysis

4-6 $\times 10^3$ cells in 100 μL were seeded in 96-well plates and left at 37°C in a 5% CO_2 atmosphere for 24 h then treated with different concentrations of complexes which were dissolved in DMSO. The complexes were dissolved in DMSO (< 1%). For cytotoxicity in dark, all complexes were treated under dark conditions, the cells were treated with the compounds for 72 h and then the mixture of 10 μL MTT (5 mg/ml) and 90 μL cell culture medium was added into each well and incubated for 2 h. After the medium was removed, 100 μL DMSO was added to dissolve the formazan crystals until the color reaction was completed. The plates were then read at $\text{OD}_{570\text{nm}}$ using a Tencan Infinite M200 microplate reader (Tencan, Swiss) and IC_{50} were calculated. The IC_{50} represents the concentration of complexes that reduces cell viability to 50%. Photo-induced cytotoxicity was also assessed under the same conditions above for detection by MTT assay according to the following procedure. The cells were seeded on 96 well plates for 24 h then treated with different concentrations of the complexes. The NCI-H460 cells were incubated with complexes for 4 h, and then irradiated with 420 nm light for 10 min (11.07 mW/cm^2) by cell photo-toxicity LED irradiators (PURI Material, China). After exposure to light irradiation, the plates were incubated for total of 72h, MTT assay was then performed by the same experiment protocol as above. Evaluation is based on means from three independent experiments, each comprising four replicates per concentration level.

Cell colony formation analysis

For colony formation assay, 1000 cells per well were plated in 6-well plates. After incubating in a constant temperature incubator for 24 h, different concentrations of **T1** (5, 10 and 20 μM) were added to the cells and cultured for 72 h. Then the medium was replaced and the cells cultured for additional 7 days. The colonies were fixed in 4% paraformaldehyde and (Beyotime, China) stained with Crystal Violet Staining Solution (Beyotime, China). Colonies were counted and image by a digital camera.

Apoptosis analysis

Apoptosis was detected using the Annexin V-FITC/PI apoptosis detection kit (BD Biosciences, USA). NCI-H460 cells (2.5×10^5 cells/well) were seeded in 6-well plates for 24h and treated with **T1** (5, 10 and 20 μM) for 48h. Then the cells were harvested, washed with ice-cold PBS (Beyotime, China) and incubated with 5 μL Annexin V-FITC and PI working solution with 100 μL 1 \times Binding Buffer for 20 min at room temperature in dark. After incubation, cells were measured and analyzed by BD C6 flow cytometry within 1 h (BD Biosciences, USA).

Reactive oxygen species analysis

The NCI-H460 cells were seeded in 6-well plate (2.5×10^5 cells/well) and incubated at 37 °C and 5% carbon dioxide for 24 hours. After exposure to **C1** (10 and 20 μM) and **T1** (10 and 20 μM) for 12 h, the cells were treated with the ROSUP (0.25 mg/mg) for 20 min. The cells were washed with no-FBS RPMI media and incubated DCFH-DA working solution (Beyotime Biotechnology, China) for 20 min in the dark at 37°C. The generation of ROS was measured by BD C6 flow cytometry (BD Biosciences, USA).

SUPPORTING INFORMATION

LDH release analysis

The NCI-H460 cells were seeded in 6-well plate (1×10^5 cells/well) and incubated at 37 °C and 5% carbon dioxide for 24 hours. After exposure to **T1** (5, 10 and 20 μ M) for 48 h, the cell membrane permeabilization was quantified an LDH Cytotoxicity Assay Kit (Beyotime, China). The absorbance at 490 nm was then measured by Tencan Infinite M200 microplate reader (Tencan, Swiss).

Hoechst 33258 staining analysis

NCI-H460 cells were plated in 6-well plates (1×10^5 cells per well) and treated with **T1** (5,10 and 20 μ M) for 48 hours. The medium was then removed, and the cells were washed with PBS for 2 times. The cells were fixed with 4% paraformaldehyde (Beyotime, China) for 15 min at room temperature, stained with Hoechst 33258 (Beyotime, China) in the dark for 5 min and washed twice with PBS. Then cells were observed and imaged under a fluorescence microscope (Zeiss, Germany).

Cellular GSH analysis

NCI-H460 cells were seeded in 6-well plates (1×10^5 cells per well) and treated respectively with **C1** (10 and 20 μ M) and **T1** (10 and 20 μ M) together with BSO [L-Buthionine-(S,R)-sulfoximine] (25 μ M) (Selleck, USA) in dark or after irradiated with a 420 nm blue LED light for 10 min (11.07 mW/cm^2), continue incubation for 48 h. The intracellular GSH was detected according to the instructions of the GSH detection kit (Beyotime, China), the absorbance at 405 nm was measured by a microplate reader (Tencan, Swiss).

Western blot analysis

NCI-H460 cells were treated with **T1** (5, 10 and 20 μ M) for 48h and were washed twice with ice-cold PBS. The cells were then lysed with cell lysis buffer for Western and IP buffer (Beyotime Biotechnology, China) on ice, and quantified with the BCA assay kit (Beyotime Biotechnology, China). The supernatant of the lysate was mixed with the SDS-PAGE protein loading buffer (Beyotime Biotechnology, China) and boiled (95°C) for 5 min and then stored at – 20 °C. Protein lysates were separated on 10 – 15% SDS-PAGE with a rainbow-colored protein molecular marker (Thermo Fisher, USA) for 1.5 h at 120 V and transferred to 0.22 μ m NC membrane (Millipore, Billerica, MA, USA) for 2 h at 250 mA. The membranes were blocked for 1 h at room temperature using 5% non-fat milk and incubated overnight at 4 °C with primary antibodies. Subsequently, the membranes incubated with secondary antibody for 1 h at room temperature. The bands were visualized using enhanced chemiluminescence (Bio-Rad, USA). GAPDH, β -actin, and α -Tubulin were used as the loading control be selected according to their separation from target proteins. The primary rabbit monoclonal antibodies Pro-Caspase 8, Cleaved Caspase 8, Pro-Caspase 9, Cleaved Caspase 9, Pro-Caspase 3, Cleaved Caspase 3, GAPDH, β -actin (Cell Signalling Technology, USA), α -tubulin(Abcam, UK), and the primary mice monoclonal antibodies GPX4 (Santa Cruz, USA) were used at 1:1000 dilutions. The secondary antibody HRP Conjugated AffiniPure Goat Anti-rabbit or Anti-mice IgG (Boster Biological Technology, China) were used at 1:5000 dilutions.

SUPPORTING INFORMATION

Animal experiments

All animal experiments strictly followed the National Standards of the People's Republic of China “Laboratory animal - Guidelines for euthanasia” (GB/T 39760-2021) and “Laboratory animal - Guideline for ethical review of animal welfare” (GB/T 35892-2018). They were approved by the Institutional Animal Care and Use Committee of Shantou University Medical College and carried out at the Animal Laboratory Center of Shantou University Medical College (Certificate NO. SYXK2022-0079). BALB/c-nu mice were purchased from Hunan SJA Laboratory Animal Company (China). Throughout the experimental procedures, we made efforts to minimize the number of animals used and alleviate any potential pain or discomfort.

In brief, a density of 2.5×10^6 NCI-H460 cells were injected subcutaneously into four or five-weeks-old BALB/c nude mice to establish xenograft-bearing mice model. When the average tumor volume reached approximately 50 – 100 mm³, tumor-bearing mice were randomized into five/three groups (n = 5 in each group) and received intravenous injection. PET (60% Polyethylene glycol, 30% ethanol and 10% Tween 80, volume ratio) (Sigma, USA) was prepared for dissolving complexes and the complex **T1/C1** solution containing 10% PET which was diluted with normal saline. For **T1**-treatment, there were Control group (10% PET), **T1** treatment groups (2 mg/kg, 4 mg/kg and 8 mg/kg) and cisplatin (3 mg/kg, positive control group) were treated for 28 days very four days and 0.2 ml of the drug was injected to each mouse through the tail vein. For **C1**-treatment, there were Control group (10% PET), **C1** treatment group (8 mg/kg) and light + **C1** (8 mg/kg) treatment group were treated for 15 days very four days and 0.2 ml of the drug was injected to each mouse through the tail vein. The tumor volume and body weight of nude mice were measured and recorded every 2 days. On the 15th day after treatment, tumor tissue, organs and blood of the mice were collected. When calculating the volume and weight of the tumors, we excluded the largest and smallest tumor groups. The tumor volumes were calculated by the formula: $\frac{1}{2} (\text{Length} \times \text{Width}^2)$. All measurements were expressed as mean \pm SD; SPSS 10.0 was used for statistical analysis.

Animal liver and kidney function analysis

Mice blood was collected and centrifuged at 4°C at 1000rpm for 10 min and the supernatant was collected and store in –80°C. The serum was used for determination of levels of Alanine aminotransferase (ALT) and aspartate aminotransferase (AST), as well as the levels of blood urea nitrogen (BUN) and creatinine (CRE). The assay kits of ALT, AST, BUN and CRE (Nanjing Jiancheng Bioengineering Institute, China) were used for different index detection. The serum samples were treated with the reagents according to the product instructions provided and the absorbance was then determined by Tencan Infinite M200 microplate reader (Tencan, Swiss) and related indexes were calculated according to the kit protocols.

Histopathological analysis

The tissues of heart, liver, spleen, lung, kidney and tumor were fixed in 4% paraformaldehyde (Beyotime, China) for 24h. After fixing, the tissues were put respectively into a centrifugal tube filled with distilled water for cleaning twice. The paraffin sections were prepared from the tissues (thickness = 5 μ m) and placed on a microscopic glass slide. The

SUPPORTING INFORMATION

tissues were deparaffinised and rehydrated under the order of xylene, ethanol and pure water. Sections were first stained with Hematoxylin (Sigma, USA) for 5 min and rinsed with water to quickly remove the dye. Sections are then stained with Eosin Y (Sigma, USA) for 15 sec, and finally sealed with neutral gum seal. Then the tissues were observed under a microscope (Nikon, Japan).

Photo-activated Anti-tumor Activity of C1 in vivo

Female BALB/c-nu Nude mice (14 –16 g in weight and 4 – 6 weeks old) were purchased from Hunan Slake Jingda Experimental Animals Co. Ltd. Nude mice were maintained under specific pathogen-free conditions. After 7 days adaption to the laboratory animal environment, the mice were subcutaneously inoculated with NCI-H460 cells suspension (3×10^6 cells/0.1mL/mouse) in the right back flank region. When the volume of tumors reached about 100 – 200mm³. NCI-H460 tumor-bearing nude mice were divided randomly into four groups (n = 3 for each group) for different treatments, i.e. Control, **C1**-8mg/kg and Light+**C1**-8mg/kg. **C1** was dissolved by 10%PET and administered within 30 min. Group **C1** was kept in dark after injected intratumorally with 8 mg/kg **C1** (50 μ L) every four days. The group Light+**C1** was injected intratumorally with 8 mg/kg **C1** (50 μ L) and then irradiated with a 420 nm blue LED light (PURI Material, China) for 30 min (166.15 mW/cm²) after 3-hour incubation. The **C1** complex was dissolved in PET diluent (60% polyethylene glycol, 30% ethanol,10% Tween 80) and then diluted in normal saline (NS). The mice body weight and tumor perpendicular diameter of tumor were measured every 2 days respectively. All nude mice were injected intratumorally every 4 days respectively and dissected after 15 days of treatment.

SUPPORTING INFORMATION

Tables

Table S1. Summary of $\nu_{N\equiv C}$ for complexes **C1** – **C3** and **T1** – **T3**.

Entry	Complex	$\nu_{N\equiv C}/\text{cm}^{-1}$
T1	<i>trans,trans,trans</i> -Ru(PBO) ₂ (MeOPhNC) ₂	2083
T2	<i>trans,trans,trans</i> -Ru(PBO) ₂ (PhNC) ₂	2077
T3	<i>trans,trans,trans</i> -Ru(PBO) ₂ (MePhNC) ₂	2073
C1	<i>cis,trans,cis</i> -Ru(PBO) ₂ (MeOPhNC) ₂	2060, 2119
C2	<i>cis,trans,cis</i> -Ru(PBO) ₂ (PhNC) ₂	2063, 2127
C3	<i>cis,trans,cis</i> -Ru(PBO) ₂ (MePhNC) ₂	2069, 2125

Table S2. Summary of crystal and structural determination data for **C3** and **T3**.

	C3	T3
Empirical Formula	C ₄₆ H ₄₂ N ₄ O ₆ Ru	C ₄₂ H ₃₀ N ₄ O ₄ Ru
Formula weight	847.9	755.77
T(°C)	173(2) K	213 K
Wavelength	0.71073 Å	0.71073 Å
Crystal system	triclinic	triclinic
Space group	P -1	P -1
a(Å)	11.0212(3)	11.7411(5)
b(Å)	11.1947(3)	12.6035(5)
c(Å)	16.5738(5)	12.8532(6)
α(°)	81.8110(10)	75.768(1)
β(°)	84.6230(10)	79.753(2)
γ(°)	73.0820(10)	66.868(1)
V(Å ³)	1933.46(9)	1688.28(13)
Z value	2	2
D _{calc} (g cm ³)	1.456	1.487
Absorption coefficient (mm ⁻¹)	0.462	0.515
F ₀₀₀	876	772
R ^a	0.0289(7213)	0.0453(4808)
R _w	0.0673(7899) ^b	0.1081(6905) ^c
Goodness of fit	1.044	1.025

$$^a R = \sum w(F_o^2 - F_{c2})^2$$

$$^b R_w = 1/[\sigma^2(F_o^2) + (0.0260P)^2 + 1.6220P], P = (F_o^2 + 2F_{c2})/3$$

$$^c R_w = 1/[\sigma^2(F_o^2) + (0.0410P)^2 + 0.8785P], P = (F_o^2 + 2F_{c2})/3$$

SUPPORTING INFORMATION

Table S3. Selected bond lengths (Å) and bond angles (°) of **T3** and **C3**.

Entry	Bond Length (Å)		Bond Angles (°)	
T3	Ru(1)-C(14)	1.986(4)	Ru(1)-C(14)-N(2)	166.2(4)
	Ru(1)-O(1)	2.074(2)	O(1)-Ru(1)-N(1)	87.61(11)
	Ru(1)-N(1)	2.084(3)	C(14)-N(2)-C(15)	164.9(4)
	C(14)-N(2)	1.164(5)		
	N(2)-C(15)	1.405(5)		
C3	Ru(1)-C(27)	1.901(2)	Ru(1)-C(35)-N(4)	173.63(19)
	Ru(1)-C(35)	1.904(2)	Ru(1)-C(27)-N(3)	178.82(19)
	Ru(1)-N(1)	2.0657(17)	O(2)-Ru(1)-N(1)	85.30(6)
	Ru(1)-N(2)	2.0683(16)	O(2)-Ru(1)-N(2)	84.77(6)
	Ru(1)-O(2)	2.1030(13)	C(35)-N(4)-C(36)	173.4(2)
	Ru(1)-O(4)	2.0835(13)	C(27)-N(3)-C(28)	177.2(2)
	N(3)-C(28)	1.396(3)		
	N(4)-C(36)	1.399(3)		
	N(3)-C(27)	1.168(3)		
	N(4)-C(35)	1.162(3)		

Table S4. ESI-MS data obtained for the photoisomerization of **C1** to **T1** after irradiated by white LED ($\lambda > 420$ nm, obtained from PRIME LED) for 15 min in DMSO/H₂O (9:1) after 30 min.

Proposed Species	Formula	Obs. <i>m/z</i>	Calc. <i>m/z</i> (exact mass)
[M – CNR + H] ⁺	C ₃₄ H ₂₄ N ₃ O ₅ Ru	656.08	656.08
[M – CNR + DMSO + H] ⁺	C ₃₆ H ₃₀ N ₃ O ₆ RuS	734.09	734.09
[M + H] ⁺	C ₄₂ H ₃₁ N ₄ O ₆ Ru	789.13	789.13
[M – CNR + 2DMSO + Na] ⁺	C ₃₈ H ₃₅ N ₃ NaO ₇ RuS ₂	834.09	834.09

Table S5. Cytotoxicity values (IC₅₀/μM) for 72h of **C1** – **C3** and **T1** – **T3** towards human cells in dark.

	C1	C2	C3	T1	T2	T3
NCI-H460	>100	>100	>100	11.8 ± 0.9	19.7 ± 3.0	36.6 ± 2.7
A549	>100	>100	>100	8.2 ± 2.2	13.3 ± 2.0	74.5 ± 9.3
MDA-MB-231	>100	>100	>100	11.6 ± 0.5	15.1 ± 1.4	53.4 ± 9.6
Hela	>100	>100	60.1 ± 8.3	8.0 ± 0.8	25.2 ± 5.4	48.5 ± 8.2
HFL1	>100	57.0 ± 11.5	45.4 ± 5.5	7.6 ± 0.7	17.2 ± 3.1	39.3 ± 2.3

SUPPORTING INFORMATION

Table S6. ESI-MS data obtained for the reaction of GSH (1 mM) with **T1** (100 μ M) in DMSO/ CH₃OH/H₂O (1:17:2) after 1 hour.

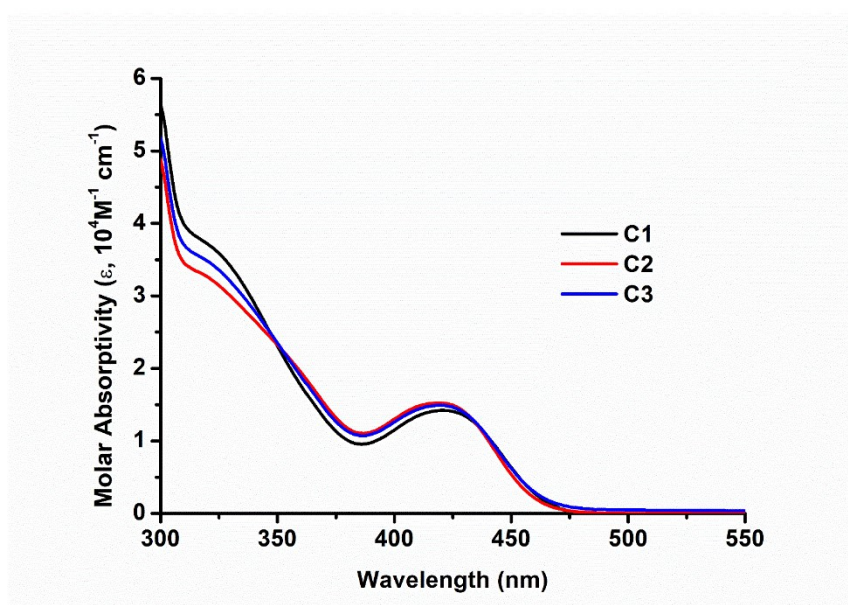
Proposed Species	Formula	Obs. <i>m/z</i>	Calc. <i>m/z</i> (exact mass)
[M – 2CNR + H] ⁺	C ₂₆ H ₁₇ N ₂ O ₄ Ru	523.02	523.02
[M – 2CNR – PBO + GSH] ⁺	C ₂₃ H ₂₅ N ₄ O ₈ RuS	619.09	619.04
[M – CNR] ⁺	C ₃₄ H ₂₃ N ₃ O ₅ Ru	655.07	655.07
[M – 2CNR – PBO + GSH + DMSO] ⁺	C ₂₅ H ₃₁ N ₄ O ₉ RuS ₂	697.10	697.06
[M] ⁺	C ₄₂ H ₃₀ N ₄ O ₆ Ru	788.13	788.12
[M – 2CNR + GSH + K] ⁺	C ₃₆ H ₃₃ KN ₅ O ₁₀ RuS	868.19	868.06

Table S7. ESI-MS data obtained for the reaction of GSH (1 mM) with **C1** (100 μ M) in DMSO/ CH₃OH/H₂O (1:17:2) after 30 min irradiation by white LED ($\lambda > 420$ nm, obtained from PRIME LED).

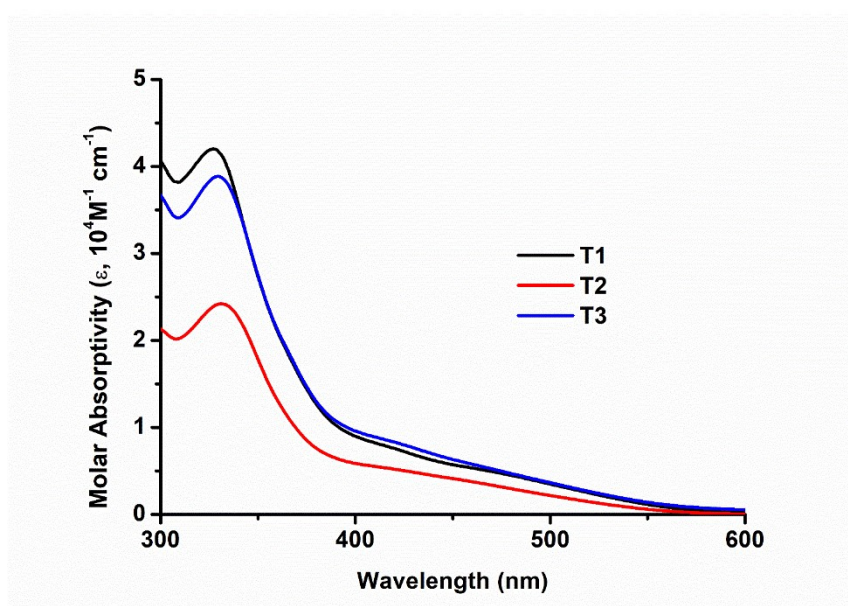
Proposed Species	Formula	Obs. <i>m/z</i>	Calc. <i>m/z</i> (exact mass)
[M – CNR + H] ⁺	C ₃₄ H ₂₄ N ₃ O ₅ Ru	656.09	656.08
[M – 2CNR – PBO + GSH – 2H + CH ₃ OH + K] ⁺	C ₂₄ H ₂₇ KN ₄ O ₉ RuS	688.10	688.02
[M – 2CNR – PBO + GSH – 2H + DMSO + K] ⁺	C ₂₅ H ₂₉ KN ₄ O ₉ RuS ₂	734.09	734.01
[M + H] ⁺	C ₄₂ H ₃₁ N ₄ O ₆ Ru	789.12	789.13
[M – 2CNR + GSH – H + K] ⁺	C ₃₆ H ₃₃ KN ₅ O ₁₀ RuS	867.15	867.05

SUPPORTING INFORMATION

Figures



(a)



(b)

Figure S1. Overlaid absorption spectra of **C1 – C3** (a) and **T1 – T3** (b) in CH_2Cl_2 .

SUPPORTING INFORMATION

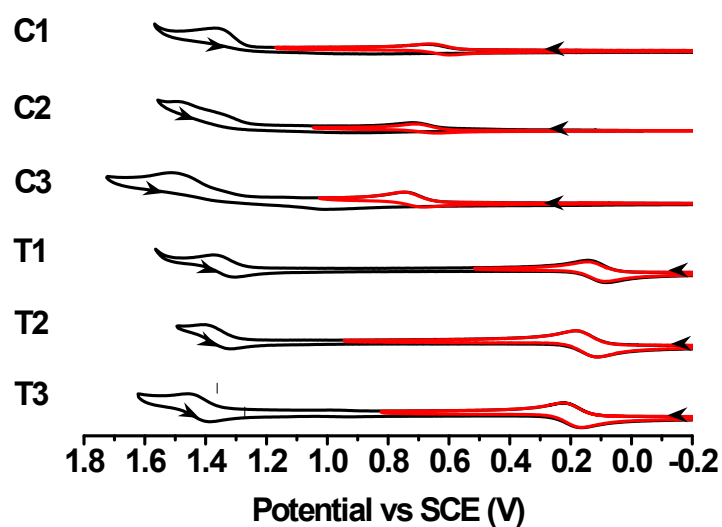


Figure S2. CVs of **C1** – **C3** and **T1** – **T3** in 0.1M [n Bu₄N]PF₆ solution in dichloromethane under Ar. Scan rate = 100 mV s⁻¹.

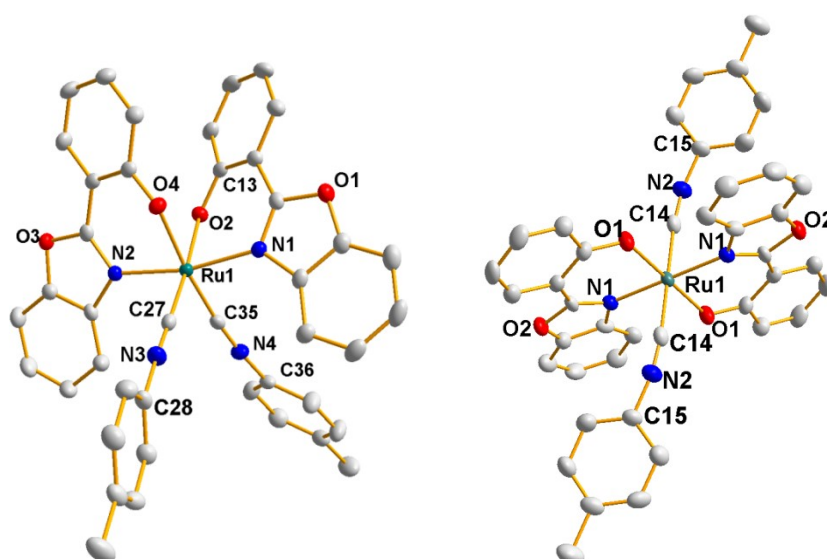


Figure S3. Perspective drawings of **C3** (left) and **T3** (right). Thermal ellipsoids are drawn at 50% probability (hydrogen atoms are omitted for clarity).

SUPPORTING INFORMATION

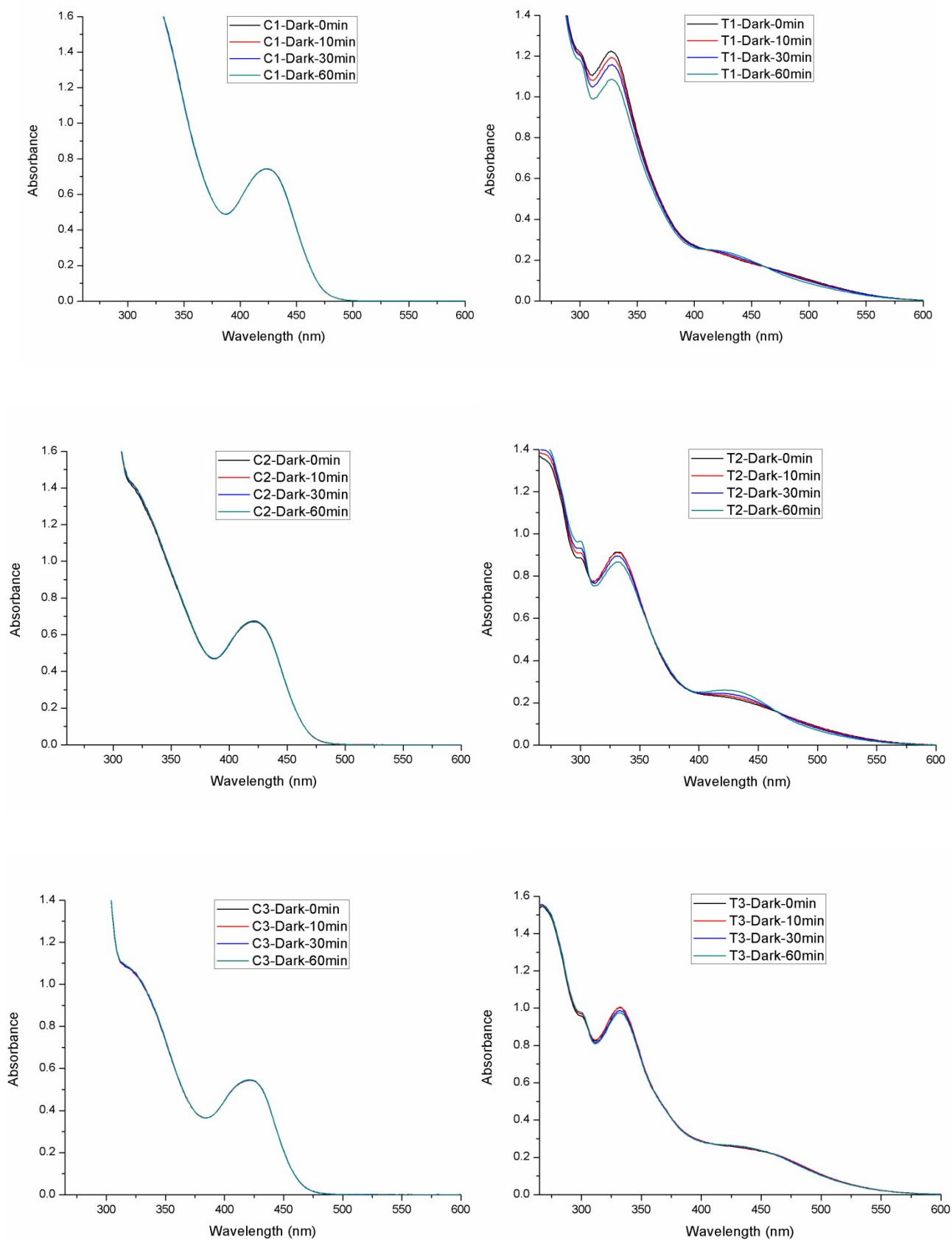


Figure S4. Absorption spectral change of 40 μ M **C1 – C3** and **T1 – T3** in DMSO in dark, respectively.

SUPPORTING INFORMATION

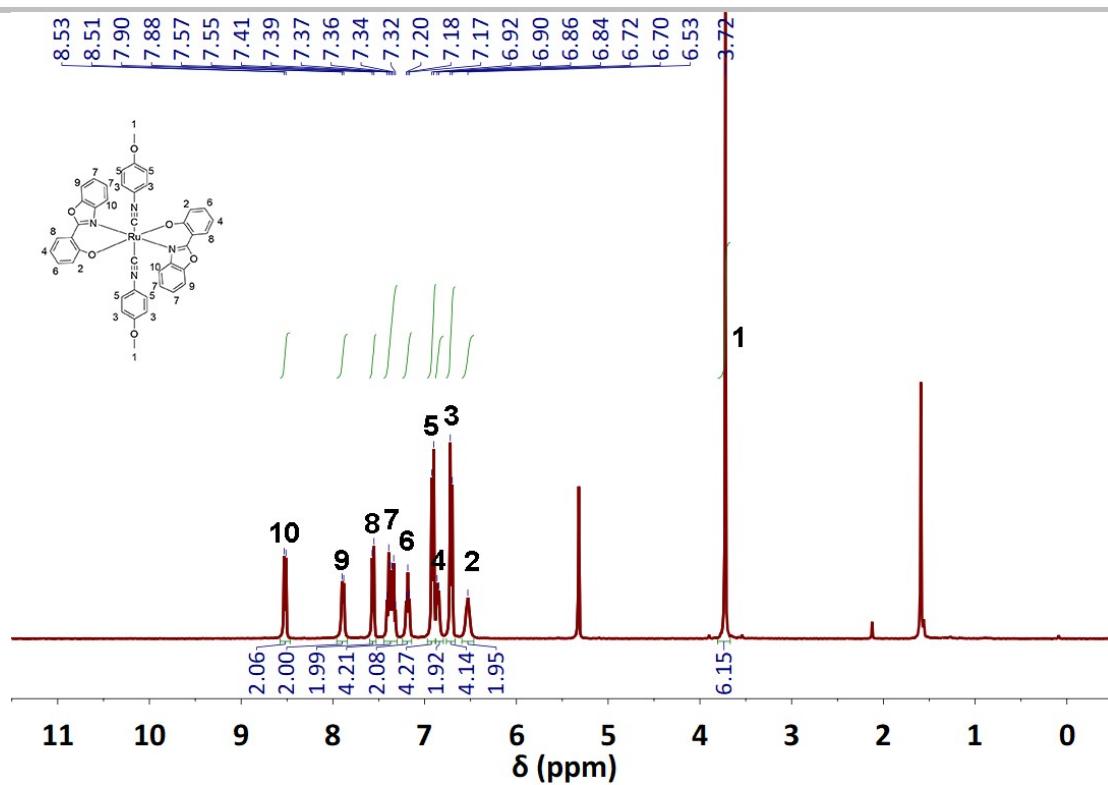


Figure S5. ^1H NMR spectrum of **T1** in d-Dichloromethane.

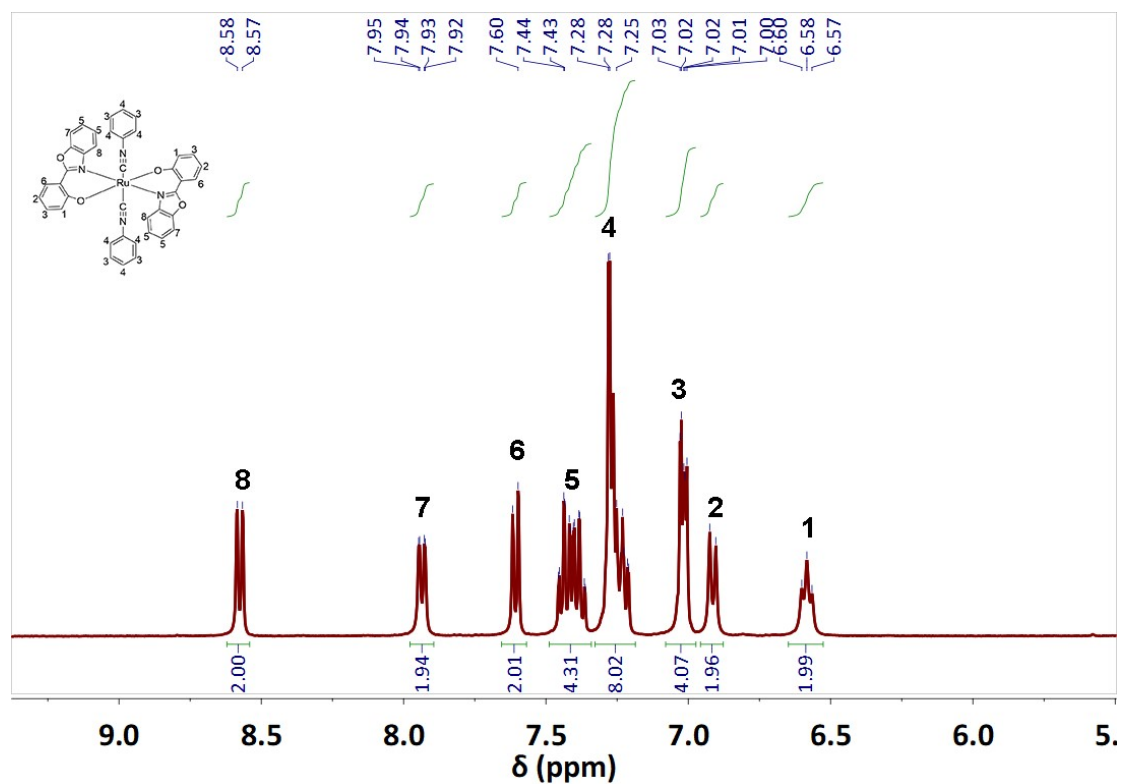


Figure S6. ^1H NMR spectrum of **T2** in d-Dichloromethane.

SUPPORTING INFORMATION

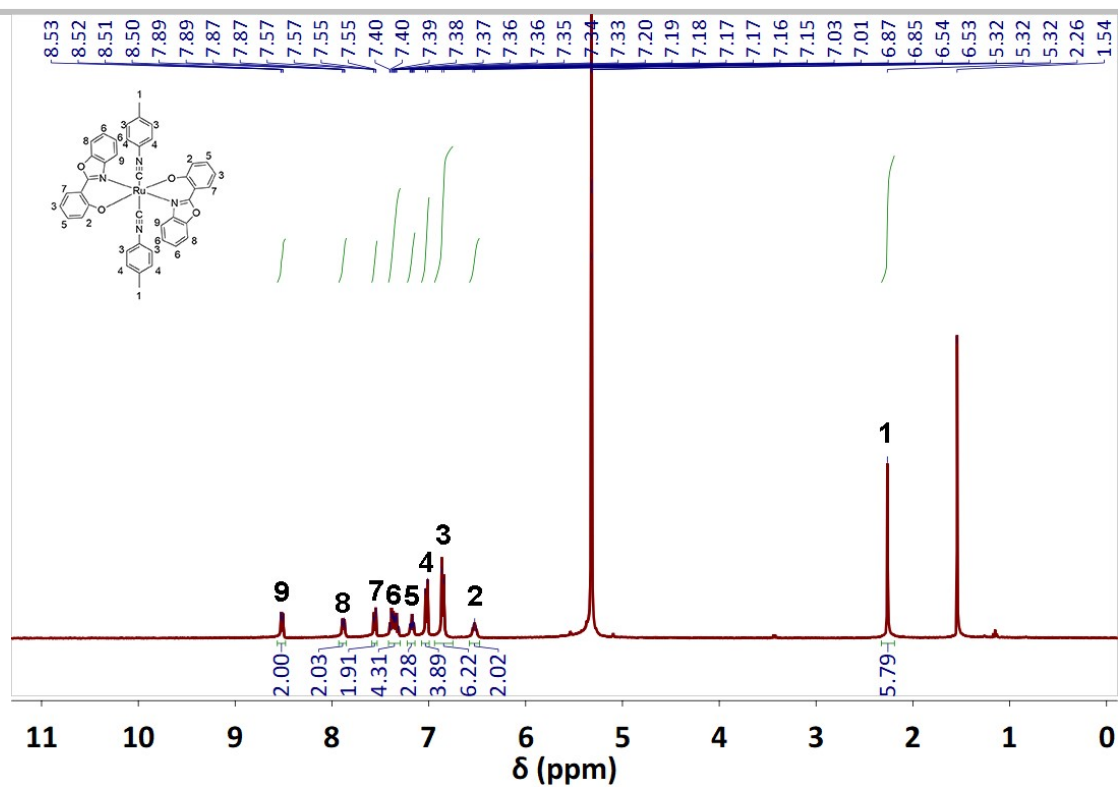


Figure S7. ¹H NMR spectrum of T3 in d-Dichloromethane.

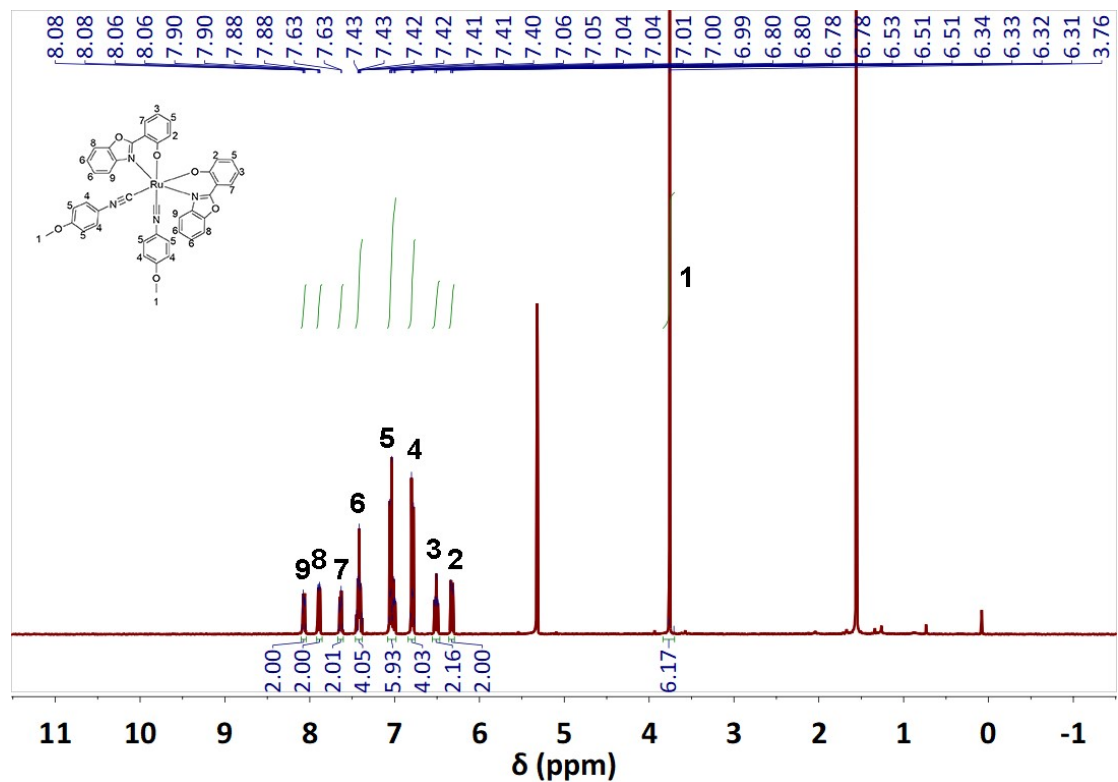


Figure S8. ¹H NMR spectrum of C1 in d-Dichloromethane.

SUPPORTING INFORMATION

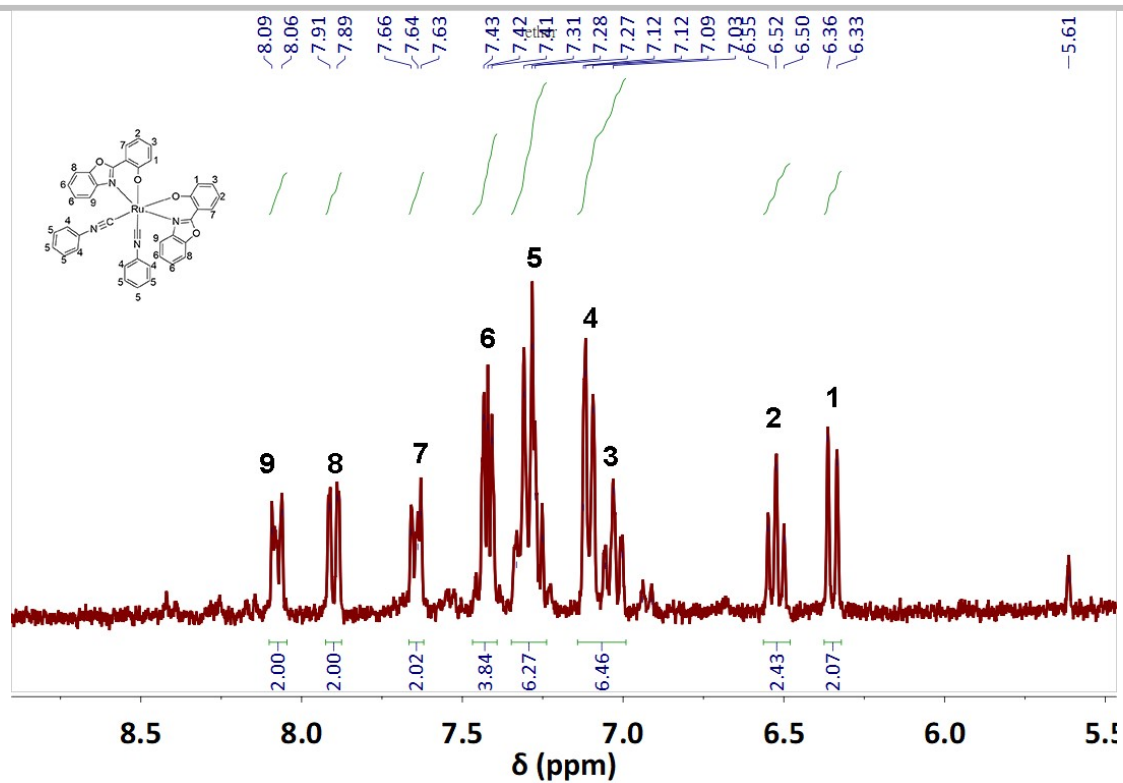


Figure S9. ¹H NMR spectrum of **C2** in d-Dichloromethane.

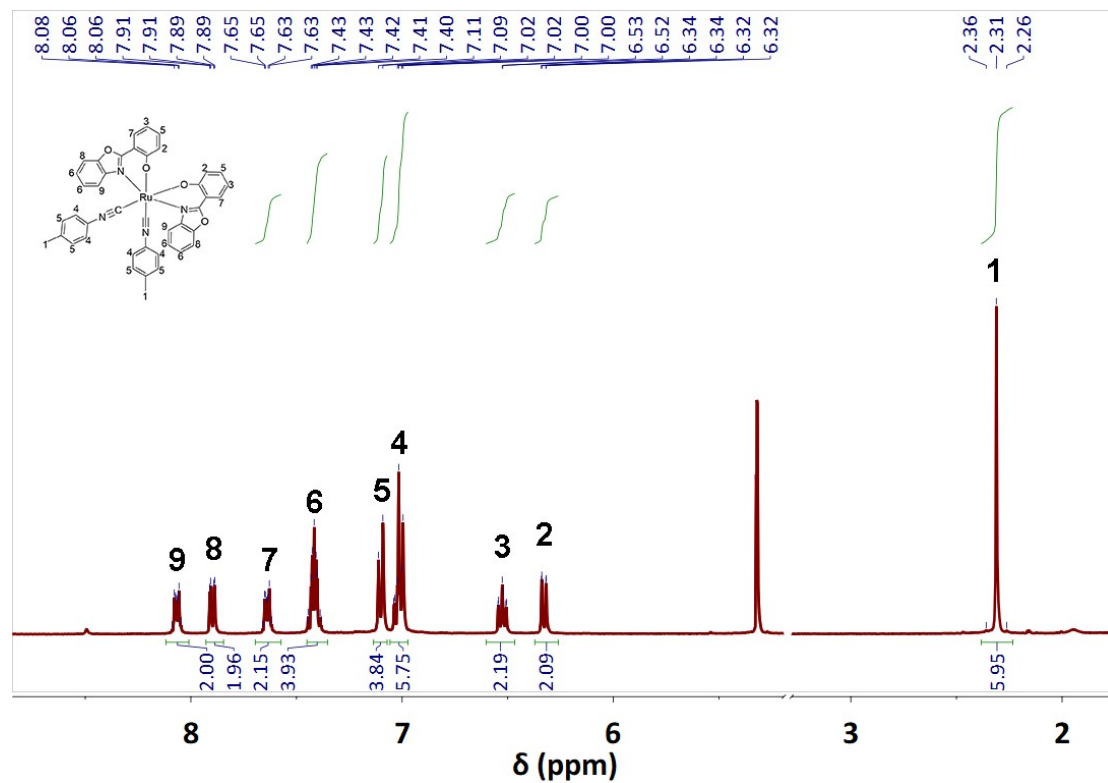


Figure S10. ¹H NMR spectrum of **C3** in d-Dichloromethane.

SUPPORTING INFORMATION

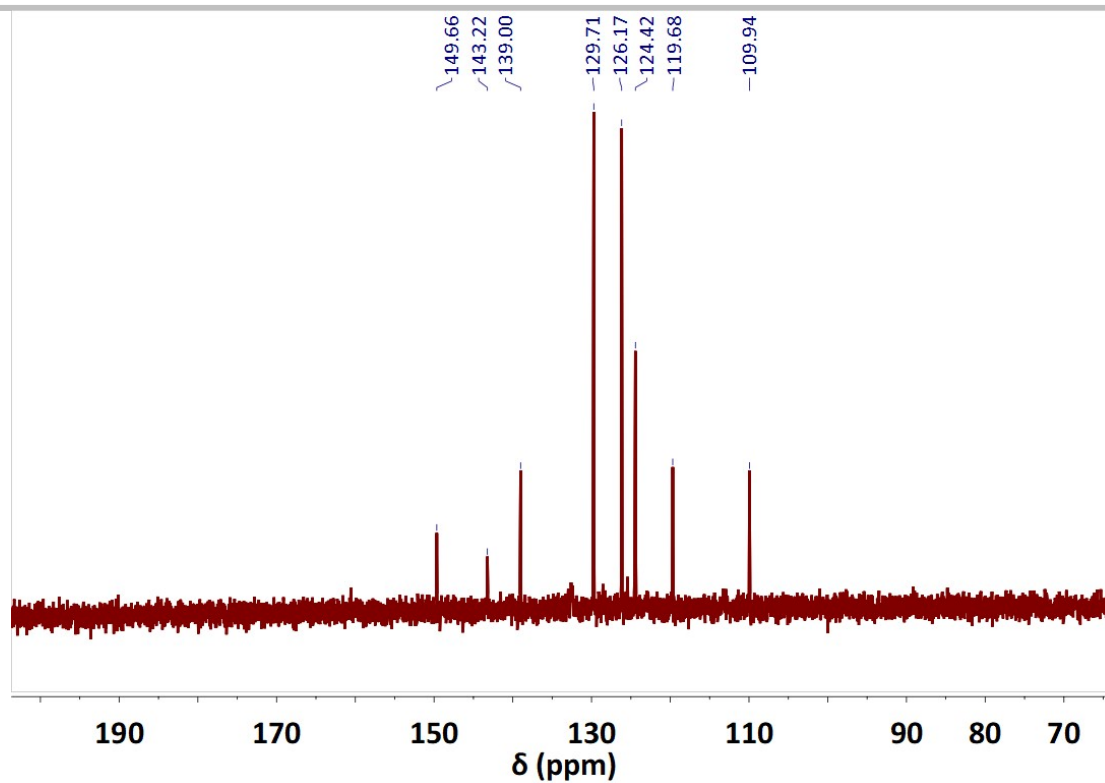


Figure S11. ^{13}C NMR spectra of **T3** in d-Dichloromethane.

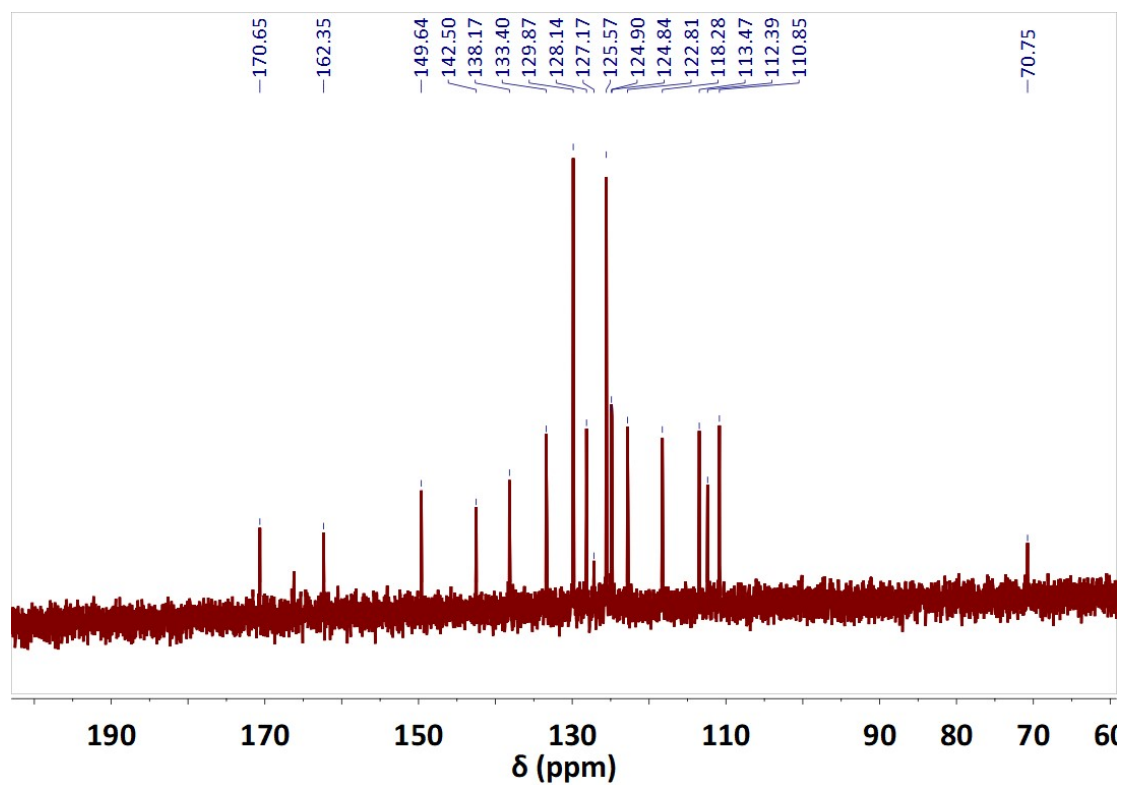


Figure S12. ^{13}C NMR spectrum of **C3** in d-Dichloromethane.

SUPPORTING INFORMATION

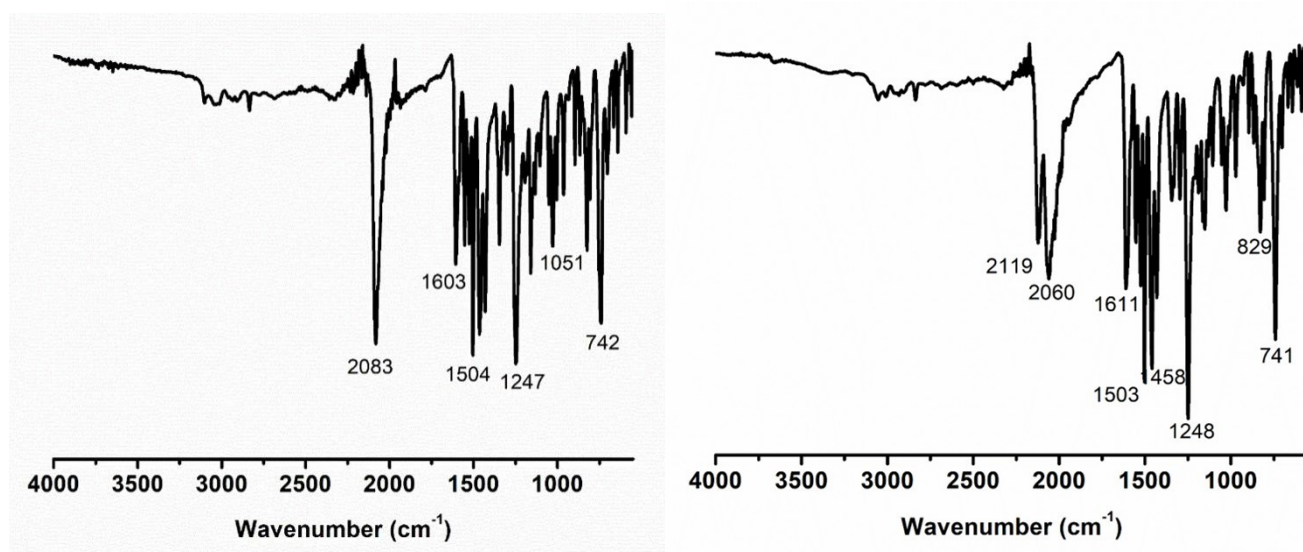


Figure S13. ATR-FTIR spectra of T1(left) and C1(right).

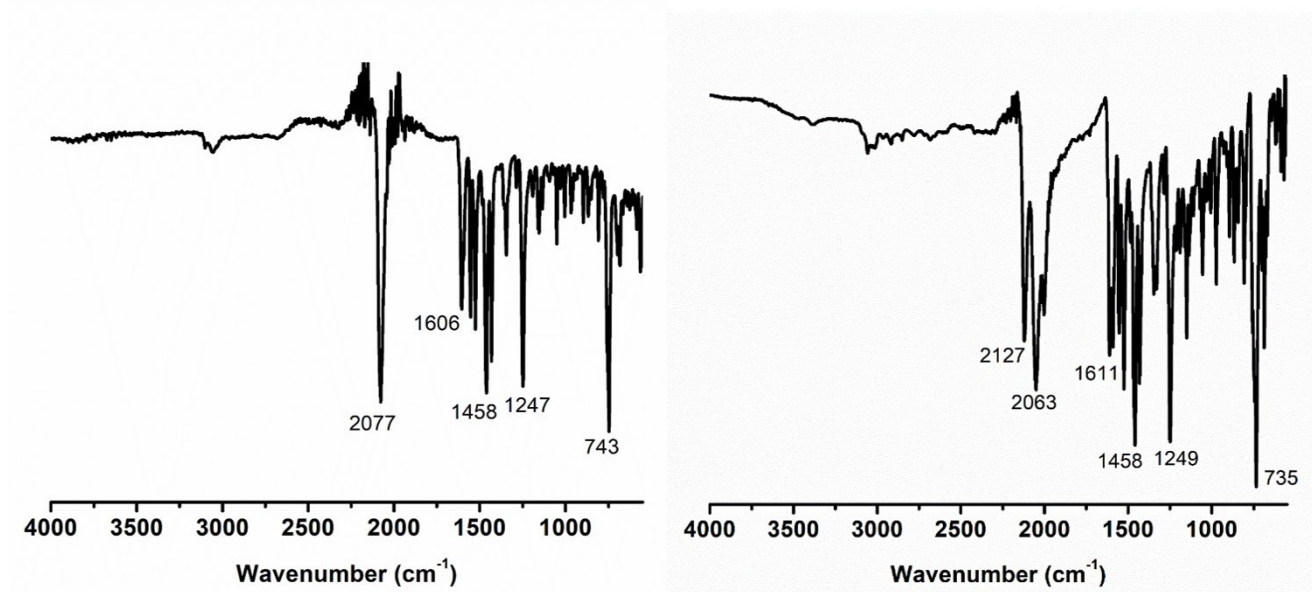


Figure S14. ATR-FTIR spectra of T2(left) and C2(right).

SUPPORTING INFORMATION

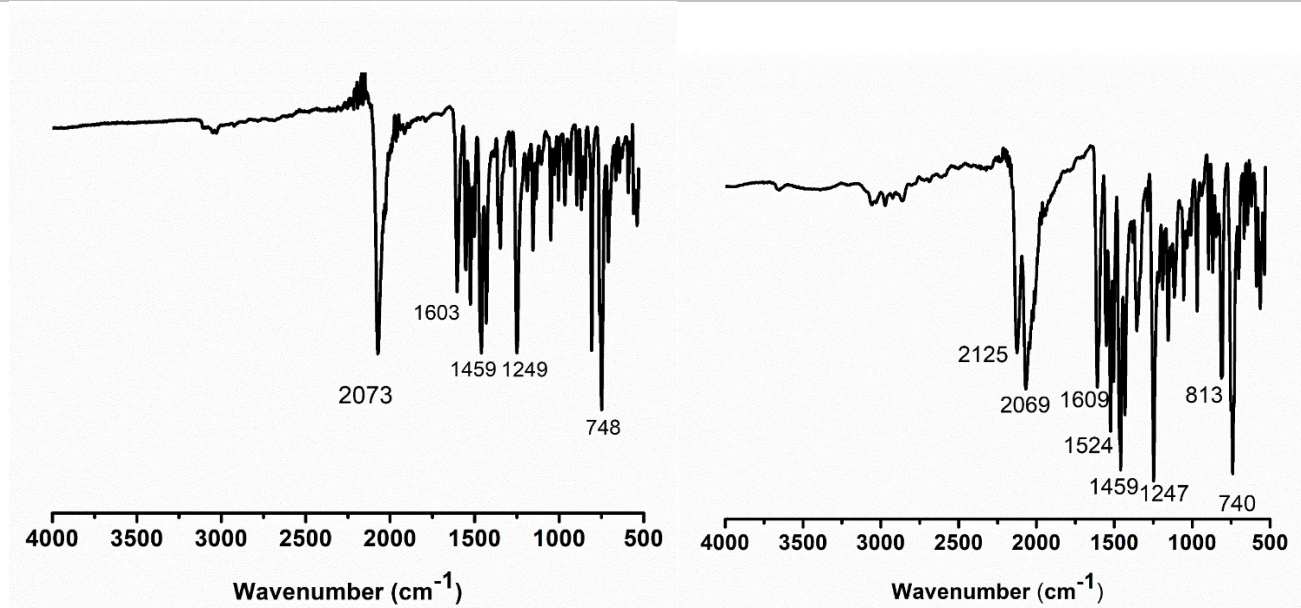


Figure S15. ATR-FTIR spectra of T3(left) and C3(right).

SUPPORTING INFORMATION

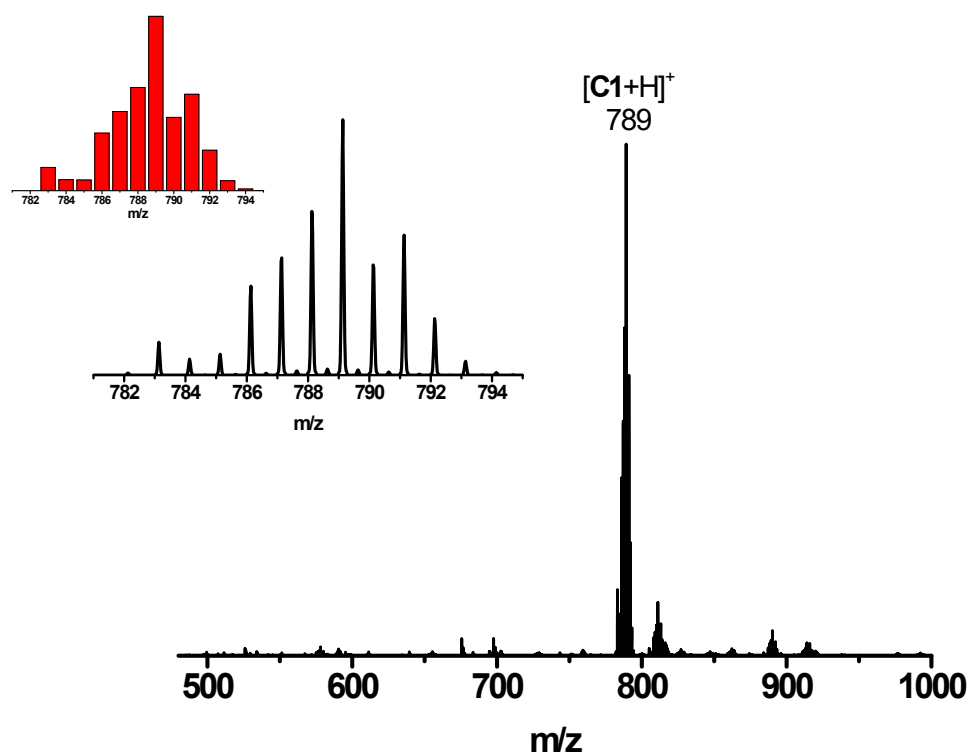
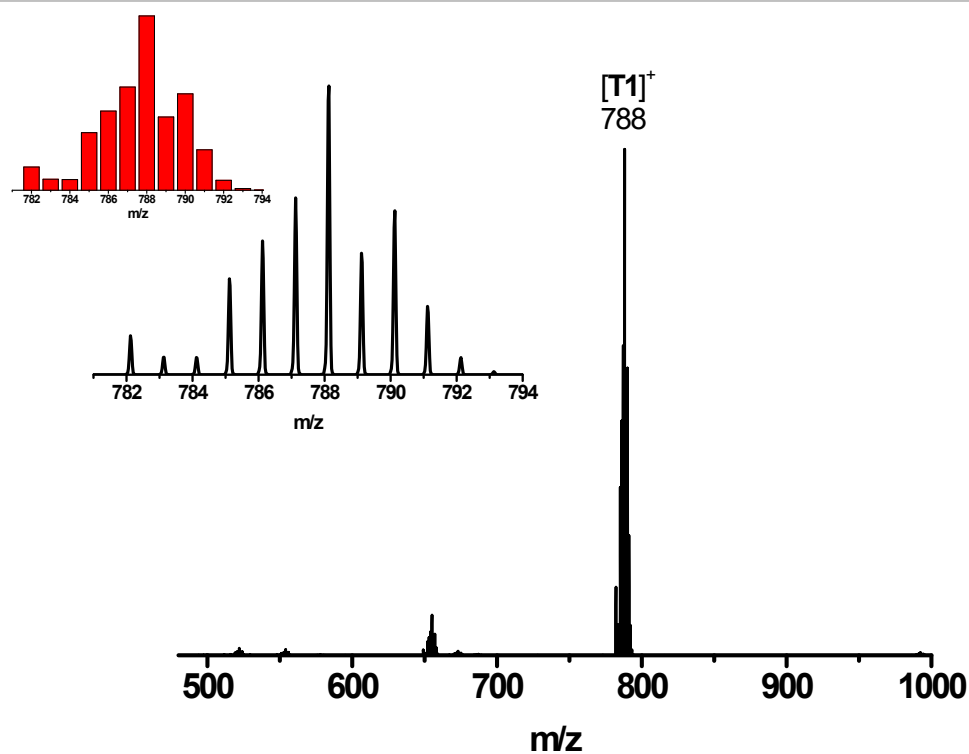


Figure S16. ESI-MS spectra of **T1** and **C1** in CH_2Cl_2 , respectively.

SUPPORTING INFORMATION

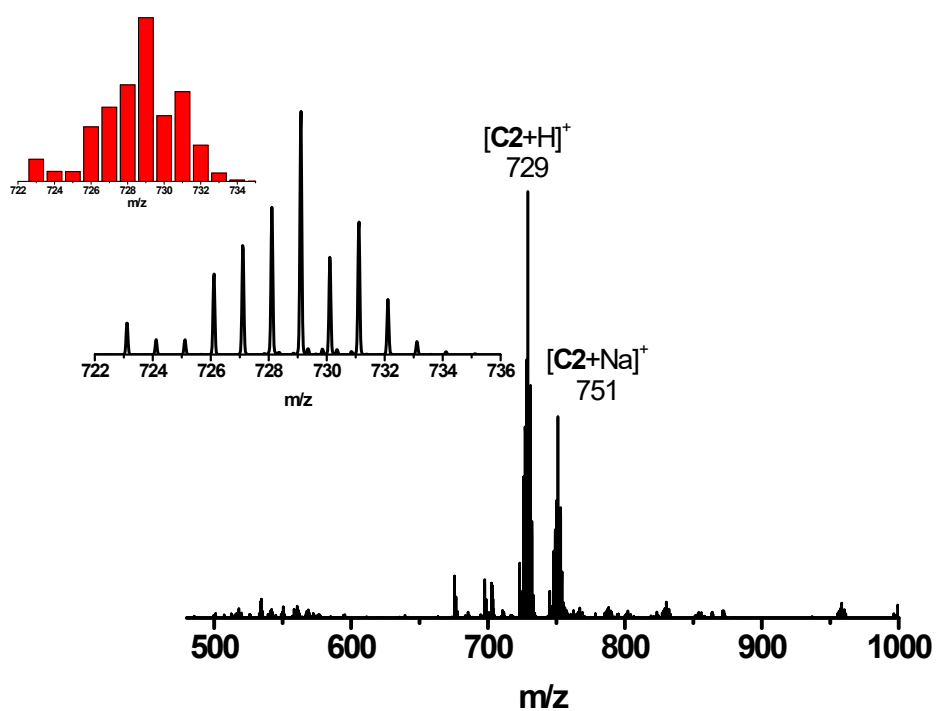
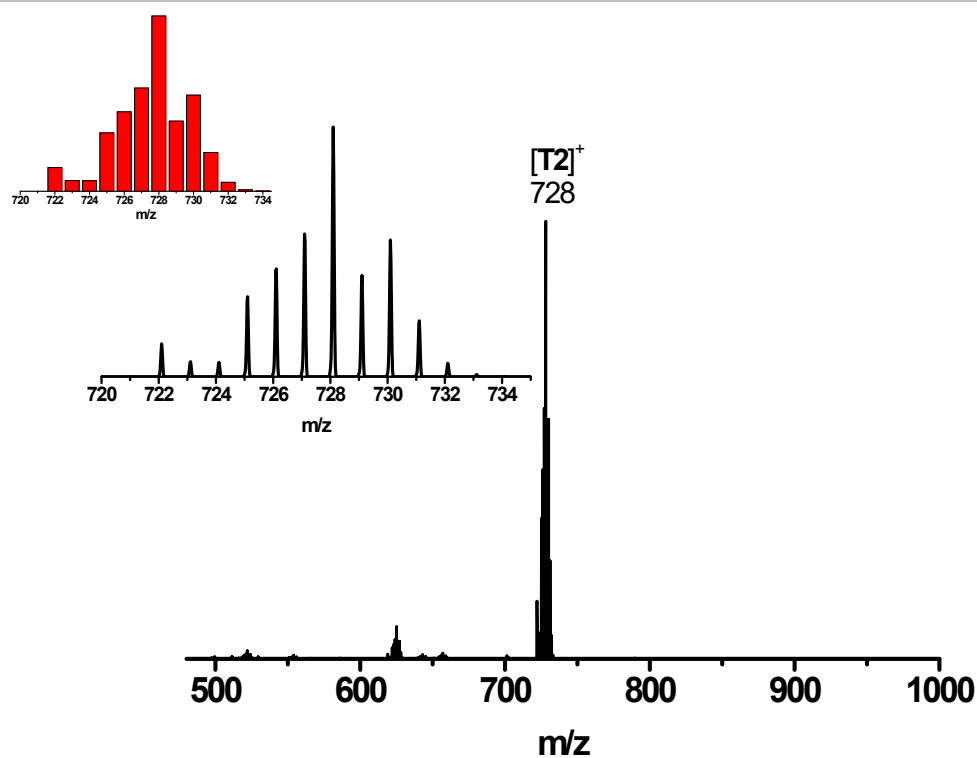


Figure S17. ESI-MS spectra of T2 and C2 in CH₂Cl₂, respectively.

SUPPORTING INFORMATION

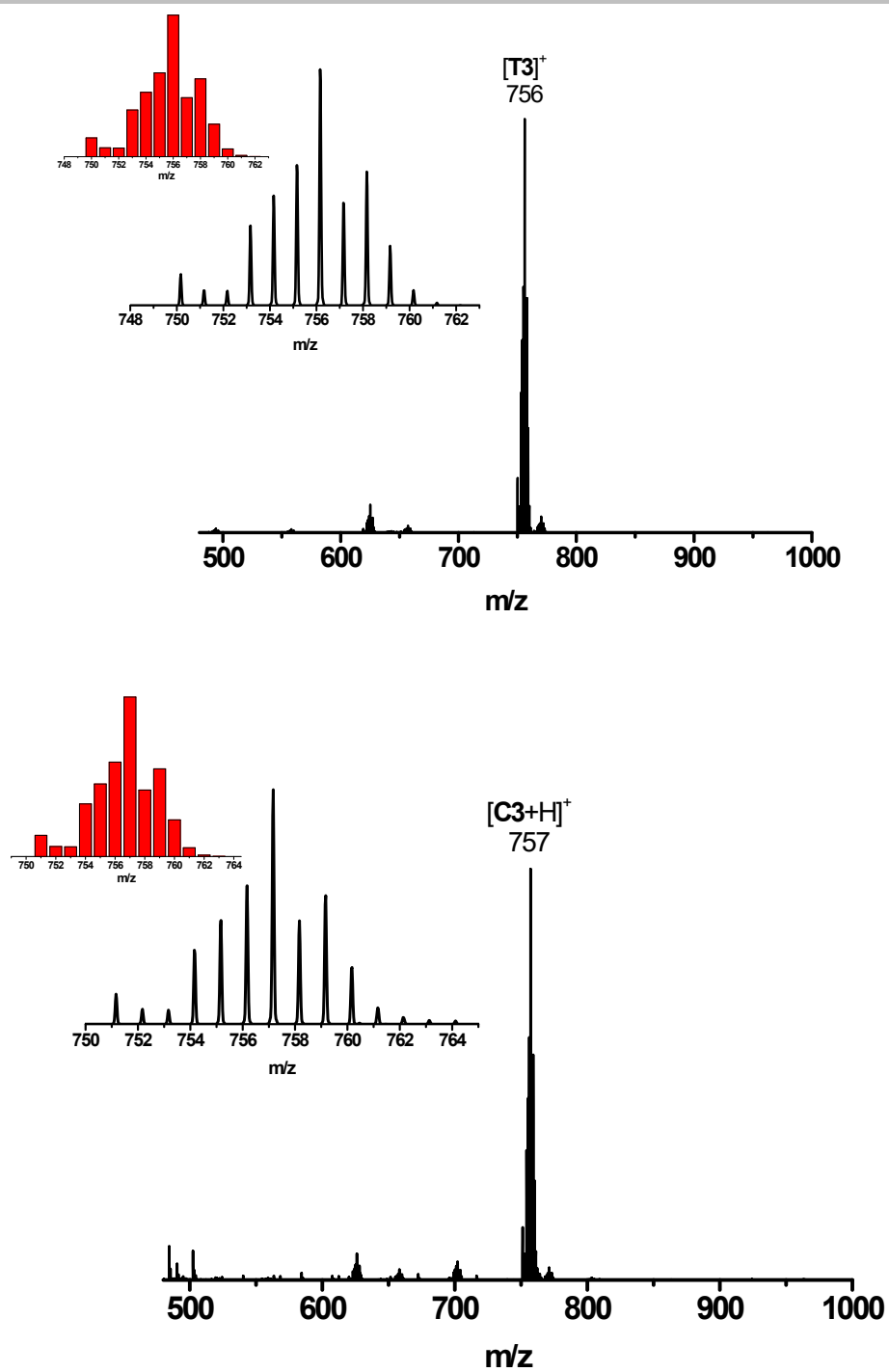


Figure S18. ESI-MS spectra of T3 and C3 in CH_2Cl_2 , respectively.

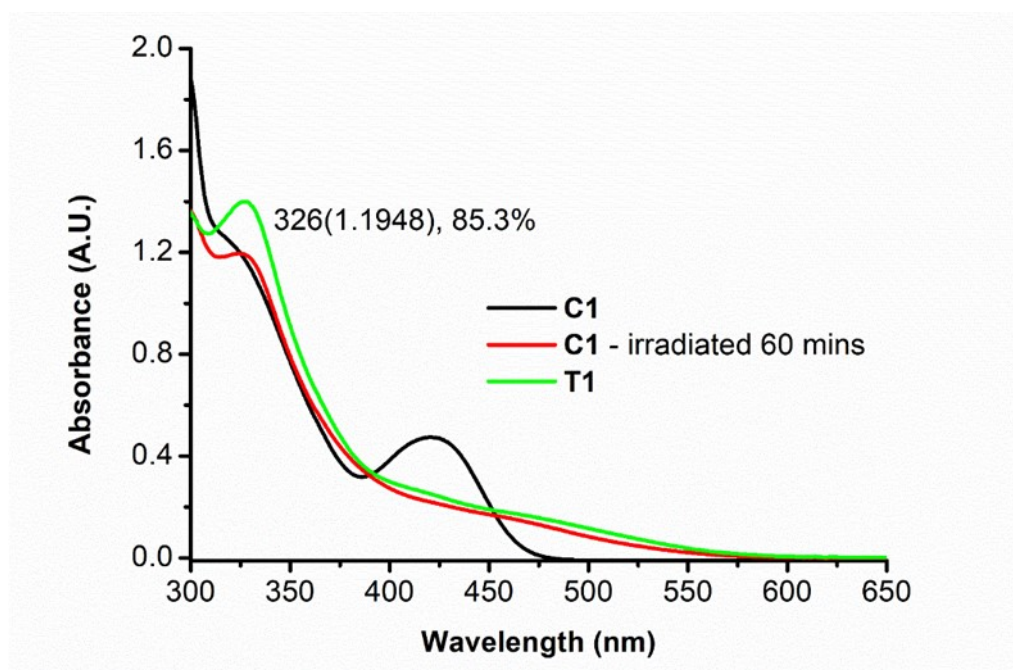
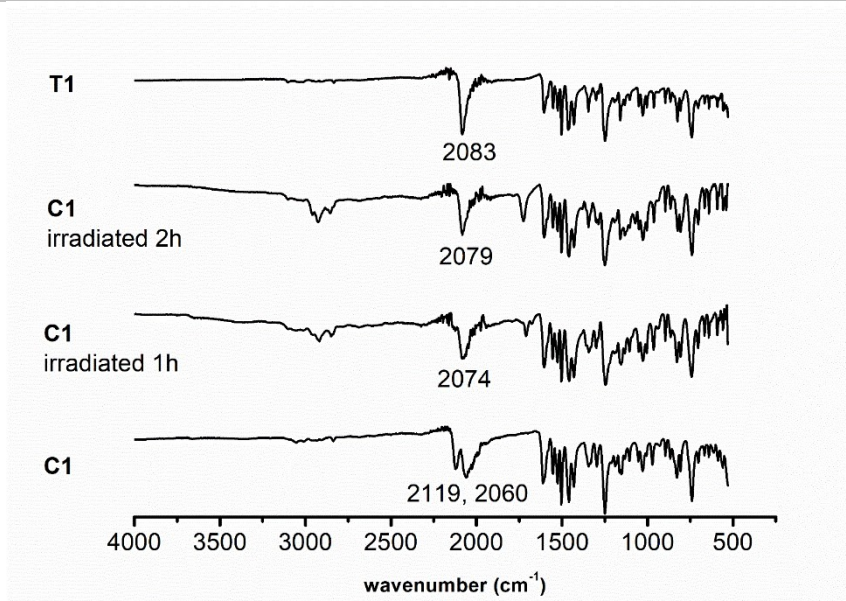
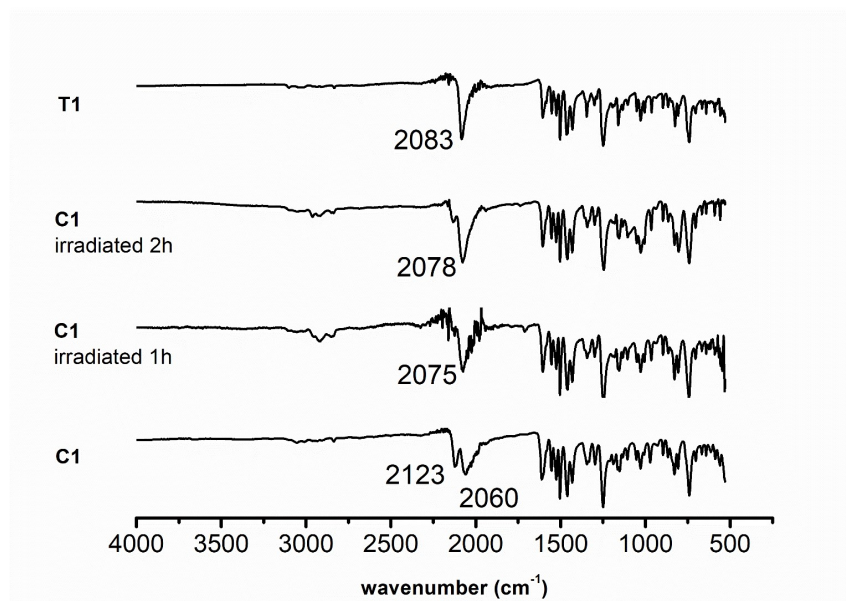


Figure S19. Overlaid UV/vis absorption spectra of **T1** (0.033 mM), **C1** (0.033mM) in CH_2Cl_2 and the product isolated from photoisomerization of **C1** after irradiation (1 hr) using white LED lamp ($\lambda > 420$ nm, obtained from PRIME LED). Percentage conversion determined by the extinction coefficient ($\epsilon = 42000 \text{ M}^{-1} \text{ cm}^{-1}$) and absorbance of peak at 326 nm (**T1**).

SUPPORTING INFORMATION



(a)



(b)

Figure S20. IR spectra of the isolated product after photoisomerization of **C1** (1 mM) in CH₂Cl₂ irradiated with white LED ($\lambda > 420$ nm, max. 471 nm, obtained from PRIME LED). under air (a) and Ar (b).

SUPPORTING INFORMATION

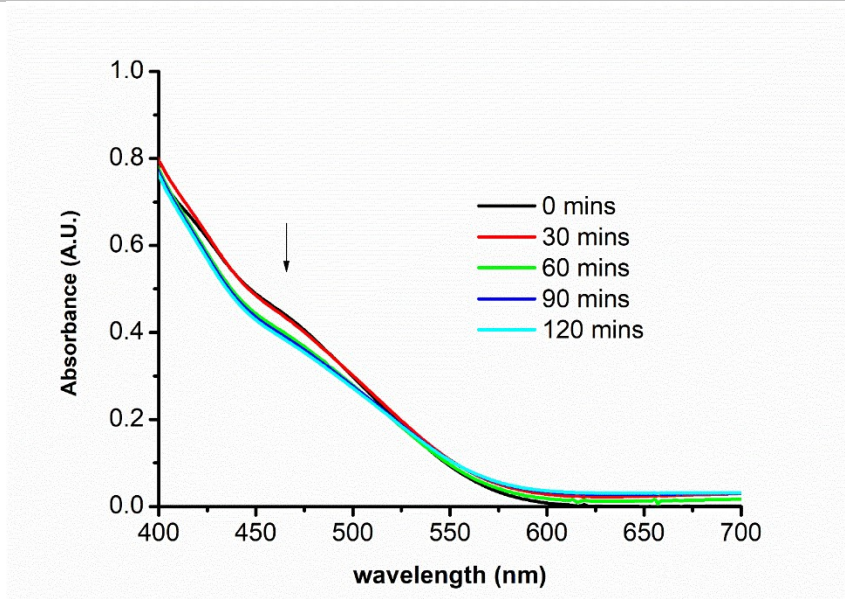
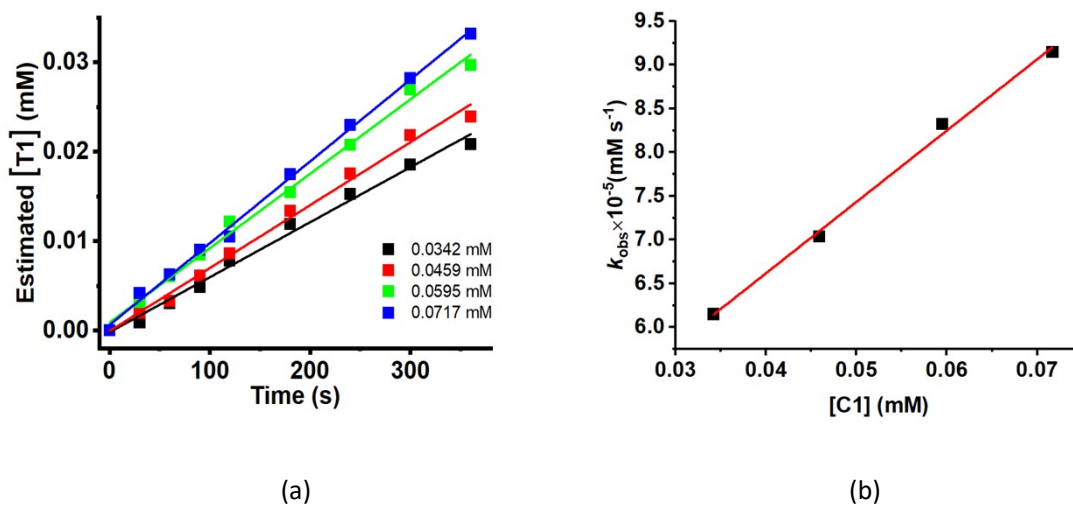


Figure S21. UV/vis absorption spectral change of **T1** (0.1 mM) in CH_2Cl_2 upon irradiation with white LED ($\lambda > 420$ nm, max. 471 nm, obtained from PRIME LED).



SUPPORTING INFORMATION

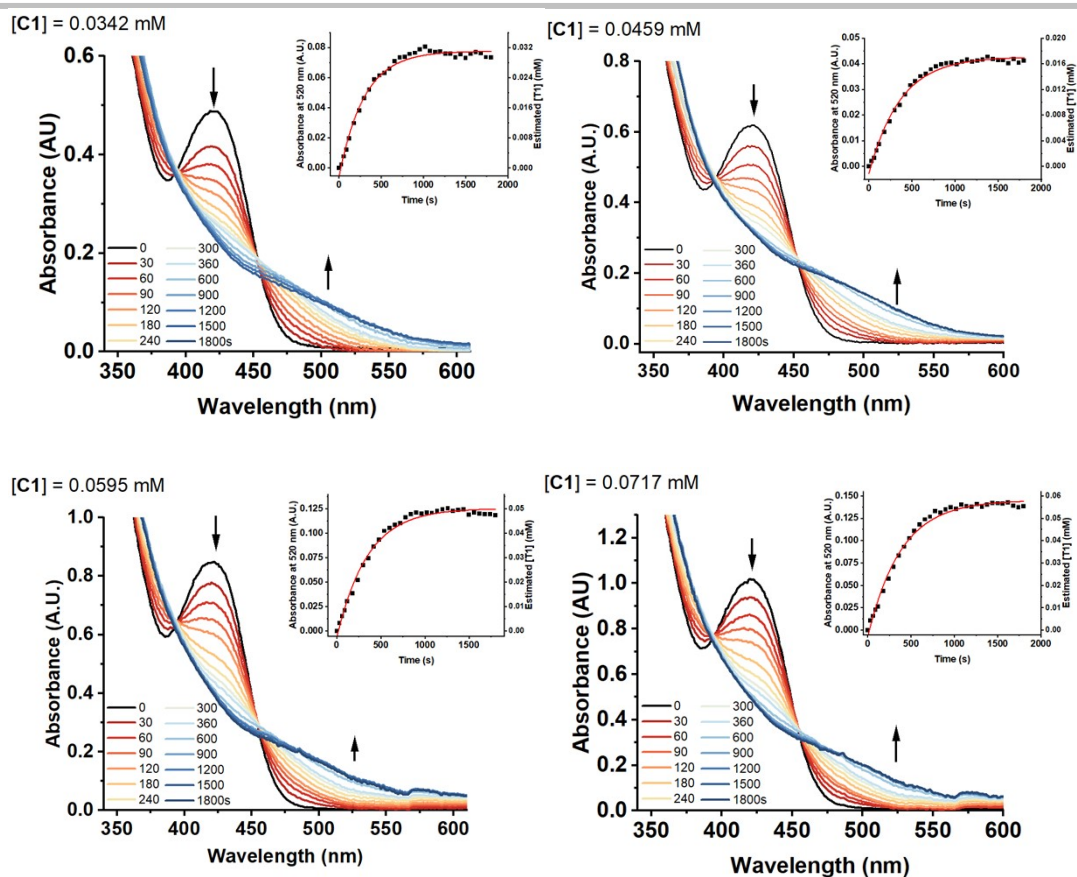


Figure S23. Spectral change of upon irradiation of **C1** (0.0342 – 0.0717 mM) in CH_2Cl_2 with white LED light ($\lambda > 420$ nm, max. 471 nm, obtained from PRIME LED). Inset: change in absorbance at 520 nm and estimated concentration **T1** produced.

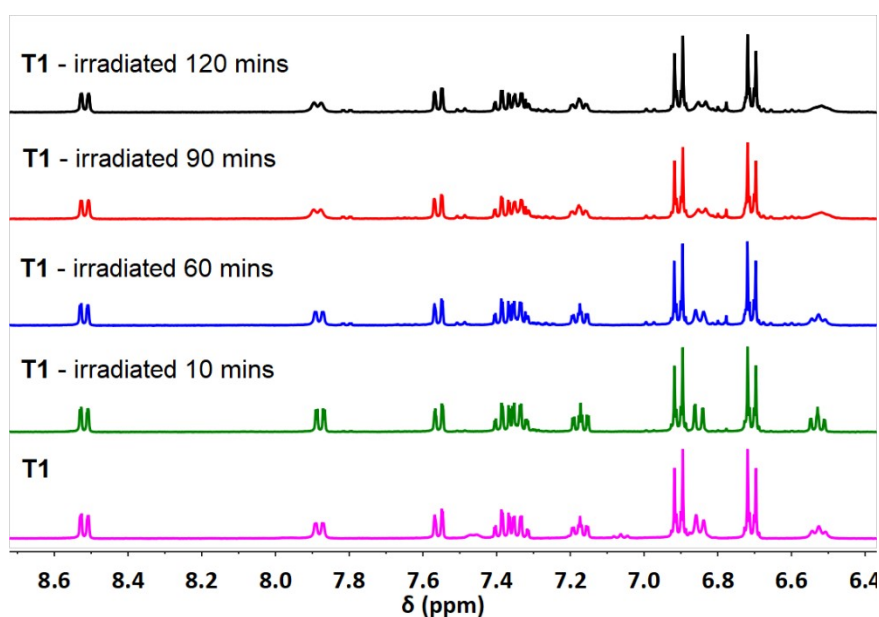


Figure S24. $^1\text{H-NMR}$ spectra of **T1** (4 mM) in CD_2Cl_2 upon irradiation with white LED ($\lambda > 420$ nm, max. 471 nm, obtained from PRIME LED) at different time (0 – 120 min) under an Ar atmosphere.

SUPPORTING INFORMATION

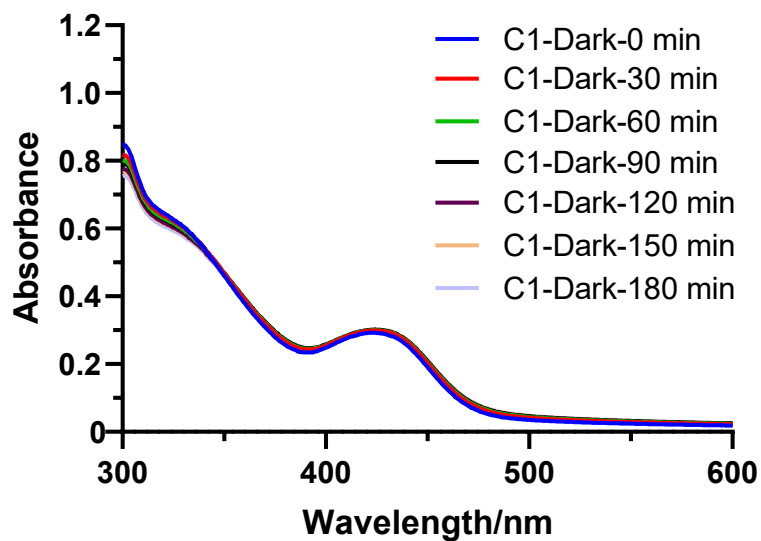


Figure S25. The absorption spectrum changes of 20 μM C1 in the dark with 5% DMSO in PBS.

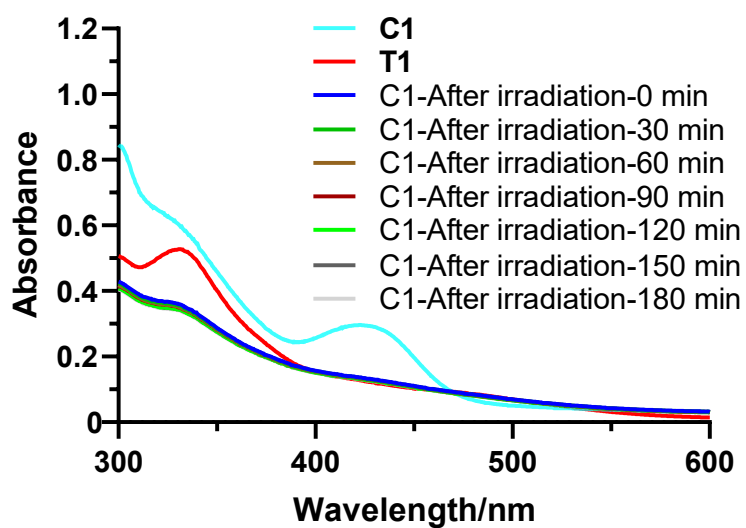


Figure S26. The absorption spectrum changes of 20 μM C1 in 5% DMSO in PBS after irradiation ($\lambda=420$ nm, 50.31 mW/cm², 40 min).

SUPPORTING INFORMATION

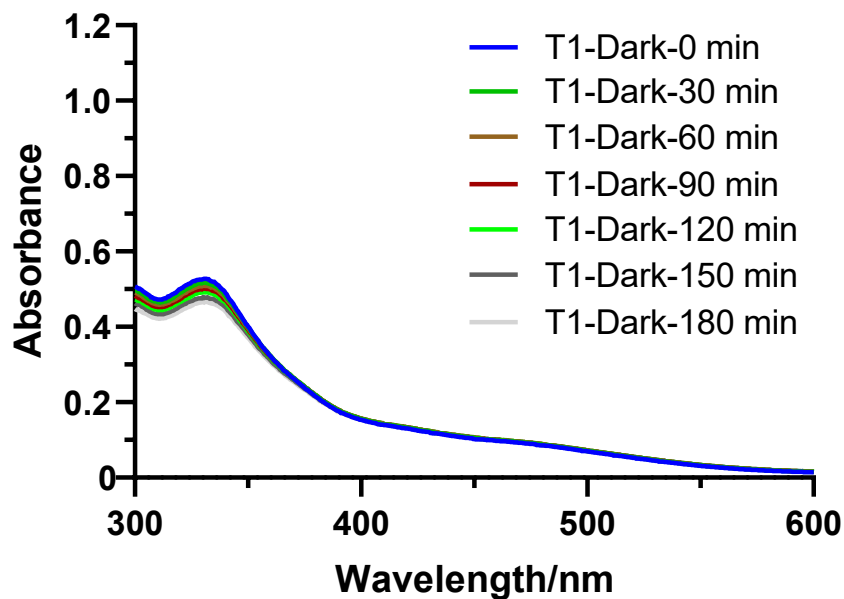


Figure S27. The absorption spectrum changes of 20 μM T1 in the dark with 5% DMSO in PBS.

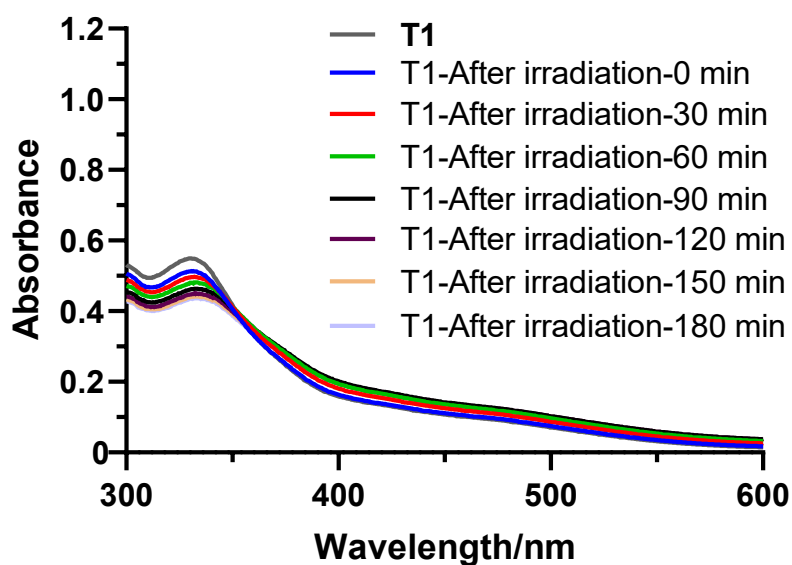


Figure S28. The absorption spectrum changes of 20 μM T1 in 5% DMSO in PBS after irradiation ($\lambda=420$ nm, 11.07 mW/cm², 10 min).

SUPPORTING INFORMATION

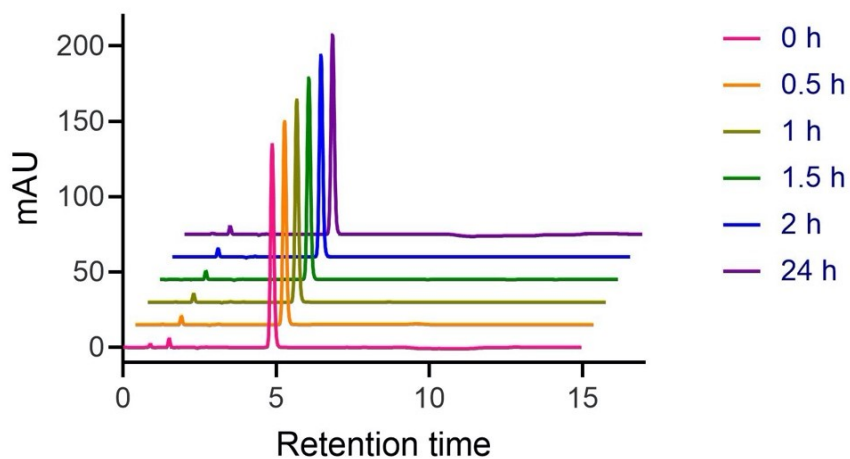


Figure S29. Stability of **C1** in mixed solvent DMSO/ACN/PBS (1:49:50, v/v/v) in the dark determined by HPLC.

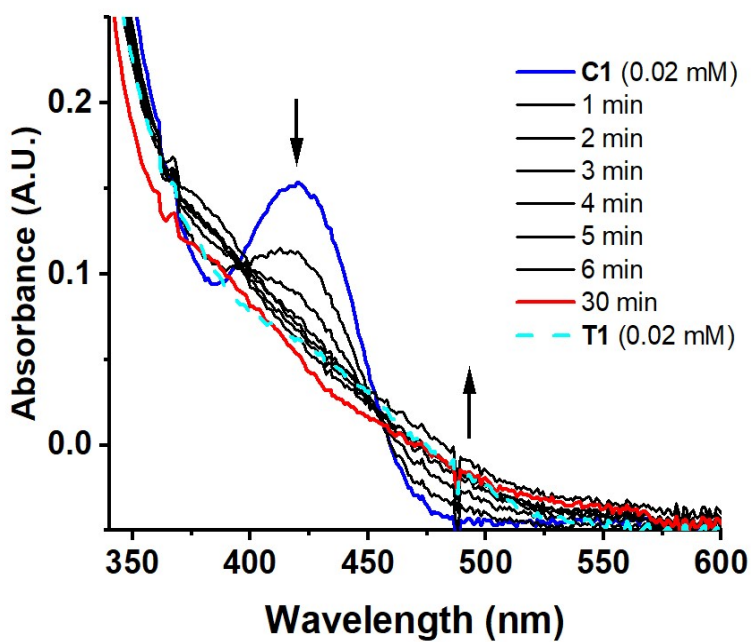


Figure S30. Spectral change upon irradiation of **C1** (0.02 mM) in DMSO/H₂O (9:1) white LED ($\lambda > 420$ nm, max. 471 nm, obtained from PRIME LED). (black line time interval = 1 min). Spectrum of **T1** (0.02 mM) (cyan dot line) after 30 min irradiation.

SUPPORTING INFORMATION

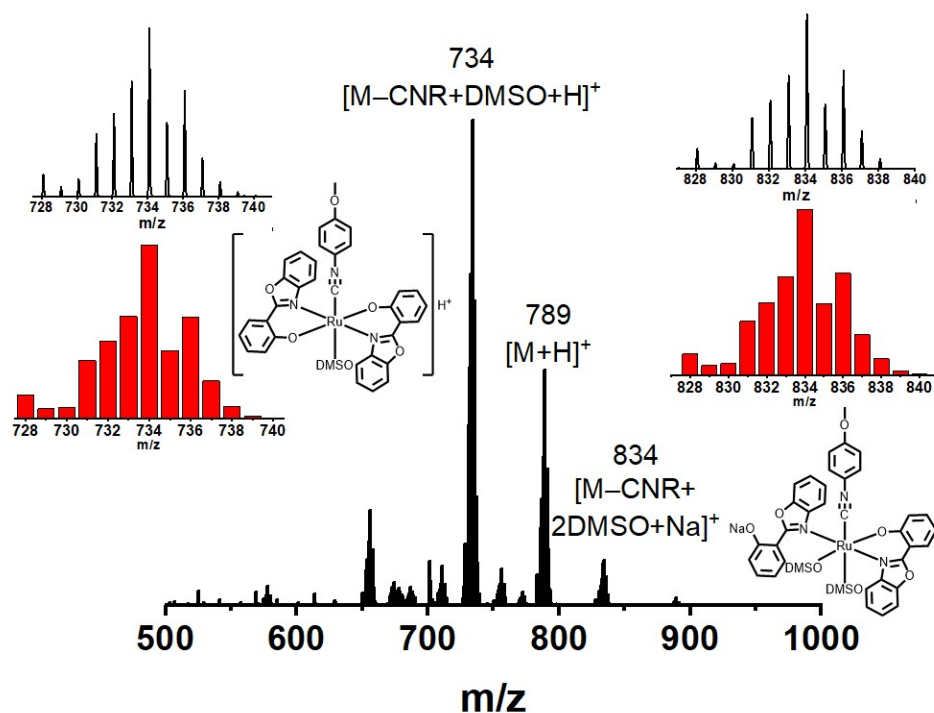


Figure S31. ESI-MS spectra of **C1** (0.02 mM) in DMSO/H₂O (9:1) after being irradiated for 30 min with white LED ($\lambda > 420$ nm, max. 471 nm, obtained from PRIME LED). Inset: simulated and experiment isotopic patterns of the peaks at $m/z = 734.09$ and 834.09 respectively.

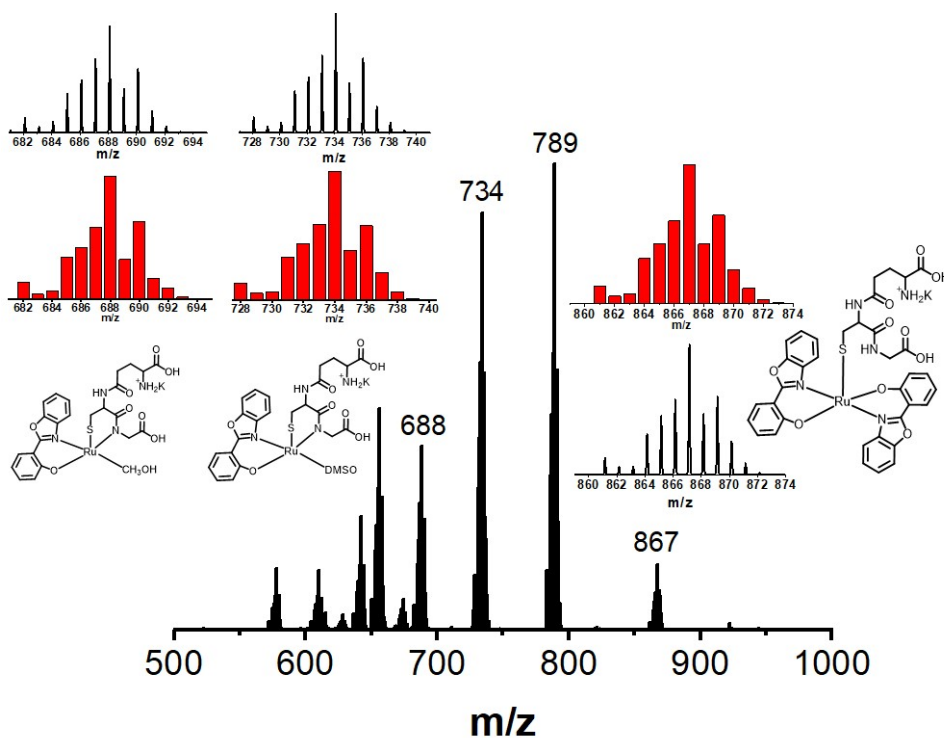


Figure S32. ESI-MS spectra of GSH (1 mM) with **C1** (0.1 mM) in DMSO/CH₃OH/H₂O (1:17:2) after being irradiated for 30 min with white LED ($\lambda > 420$ nm, max. 471 nm, obtained from PRIME LED). Inset: simulated and experiment isotopic patterns of the peaks at $m/z = 867.09$, 734.09 and 688.10 respectively.

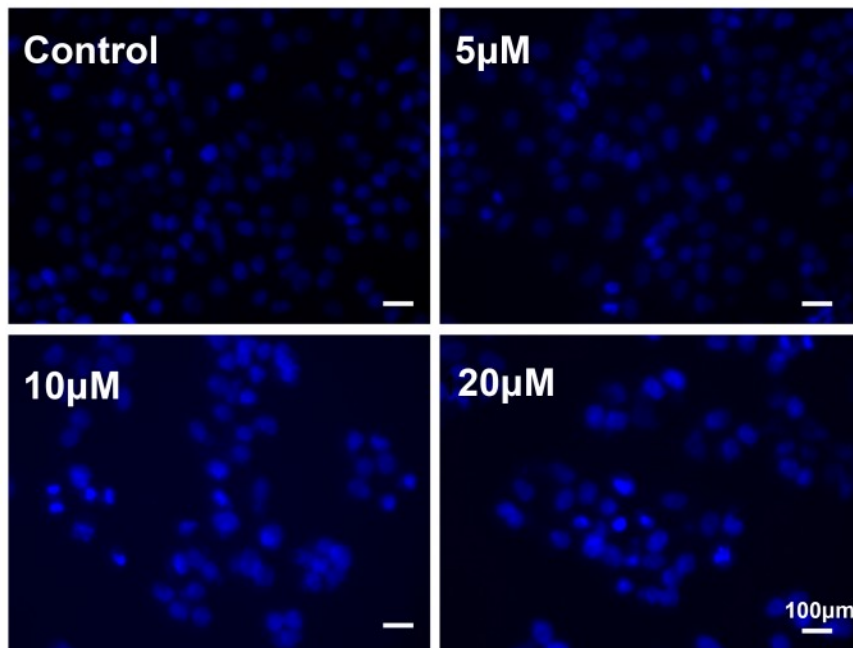


Figure S33. Staining of NCI-H460 cells with Hoechst 33258 after treatment with T1(5, 10 and 20 μ M) for 48h and were imaged by ZEISS Observer A1 microscope. (Scale bar=100 μ m)

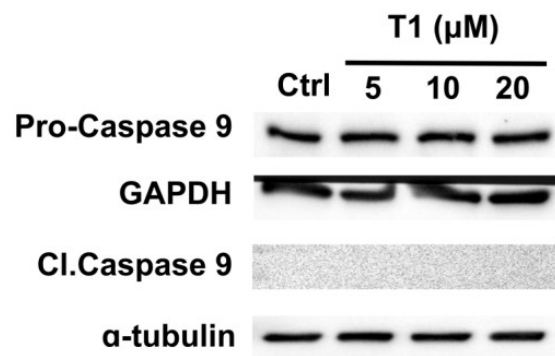


Figure S34. The expression levels change of protein of NCI-H460 cells after treatment with T1(5, 10 and 20 μ M) for 48 h by western blot assay.

SUPPORTING INFORMATION

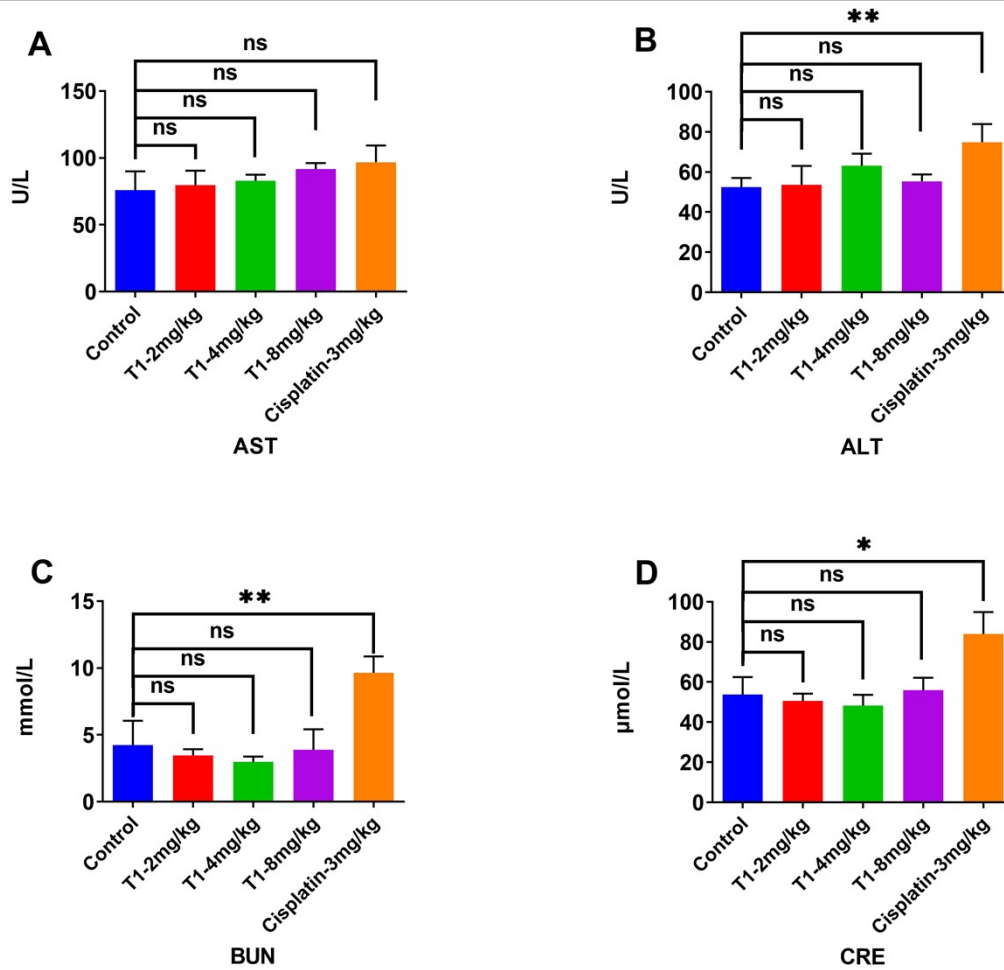


Figure S35. Effect of T1 on liver and kidney function in the BALB/c nude mice xenograft model. The levels of AST, ALT, BUN and CRE were detected by serum. (A) AST. (B) ALT. (C) BUN. (D) CRE. The data are shown as means \pm SD. * $p < 0.05$, ** $p < 0.01$, ns $p > 0.05$ vs control group.

SUPPORTING INFORMATION

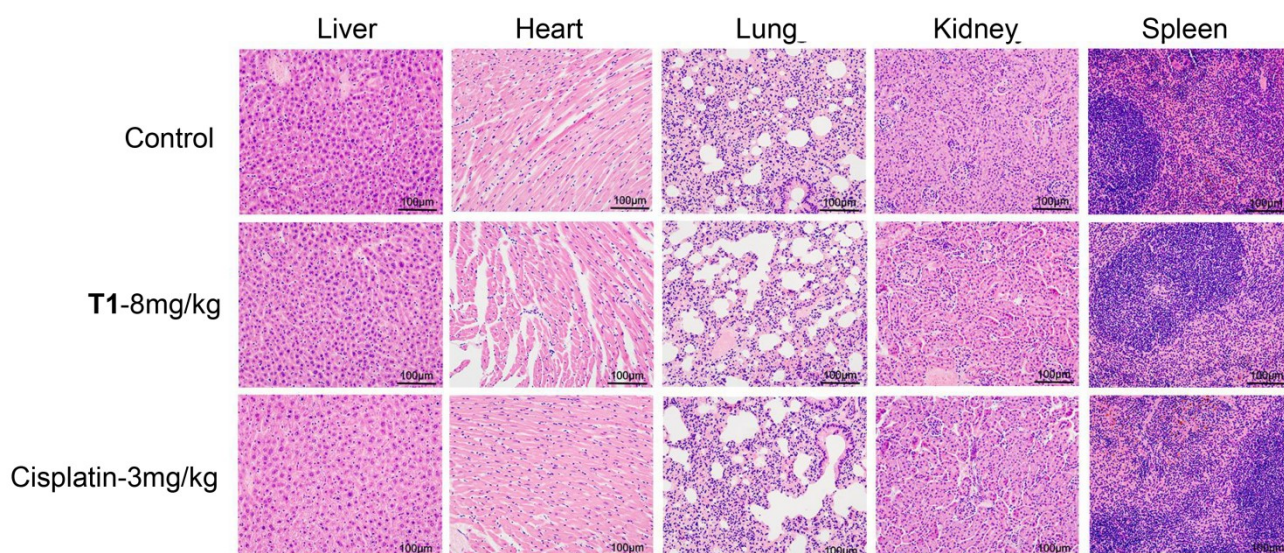


Figure S36. The effect of **T1** on the histopathologic changes of mice organ tissues was evaluated by H&E staining. Representative images of liver, heart, lung, kidney and spleen of mice in control group, **T1** treatment group (8 mg/kg) and cisplatin treatment group (3 mg/kg). (Scale bar=100 µm)

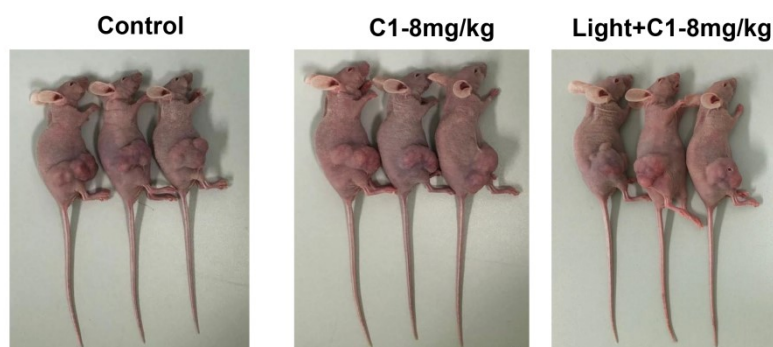


Figure S37. Photo-activate anti-tumor activities in vivo. Representative photos of mice bearing NCI-H460 cells after treatment with **C1**.

References

- 1 P.-Y. Ho, S.-C. Cheng, S.-M. Yiu, V. K.-M. Au, J. Xiang, C.-F. Leung and C.-C. Ko, *Inorg. Chem.*, 2019, **58**, 11372-11381.
- 2 L. Krause, R. Herbst-Irmer, G. M. Sheldrick and D. Stalke, *J. Appl. Crystallogr.*, 2015, **48**, 3-10.
- 3 G. M. Sheldrick, *Acta Crystallogr C Struct Chem.*, 2015, **71**, 3-8.